Novel Design of Artificial Ecosystem Optimizer for Large-scale Optimal Reactive Power Dispatch Problem with appl...

Souhil MOUASSA

Springer

Novel Design of Artificial Ecosystem Optimizer for Large-scale Optimal Reactive Power Dispatch Problem with application to Algerian Electricity Grid

Souhil MOUASSA[*, a,b,c], Francisco Jurado[a], Tarek Bouktir[b], Muhammad Asif Zahoor Raja[d, e]

[a] Department of Electrical Engineering, University of Jaén, 23700 EPS Linares, Jaén, Spain
[b] Department of Electrical Engineering, University of Farhat Abbas, Sétif 1, Algeria
[c] Department of Electrical Engineering, University of Bouira, Algeria
E-mail addresses: souhil.mouassa@univ-bouira.dz, tbouktir@gmail.com, fjurado@ujaen.es, rajamaz@yuntech.edu.tw
[d] Future Technology Research Center, National Yunlin University of Science and Technology, 123 University Road, Section 3, Douliou, Yunlin 64002, Taiwan, R.O.C.
[e] Department of Electrical and Computer Engineering, COMSATS University Islamabad, Attock Campus, Attock, Pakistan
[*] Corresponding author

Abstract – Optimization of reactive power dispatch (ORPD) problem is a key factor for stable and secure operation of the electric power systems. In this paper, a newly explored nature-inspired optimization through artificial ecosystem optimization (AEO) algorithm is proposed to cope with ORPD problem in large-scale and practical power systems. ORPD is a well-known highly complex combinatorial optimization task with nonlinear characteristics and its complexity increases as number of decision variables increase, which makes it hard to be solved using conventional optimization techniques. However, it can be efficiently resolved by using nature-inspired optimization algorithms. AEO algorithm is a recently invented optimizer inspired by the energy flocking behavior in a natural ecosystem including in non-living elements such as sunlight, water and air. The main merit of this optimizer its high flexibility that leading to achieve accurate balance between exploration and exploitation abilities. Another attractive property of AEO is that it does not have specific control parameters to be adjusted. In this work, 3-objectives version of ORPD problem are considered involving active power losses minimization and voltage deviation (VD), and Voltage stability index (VSI). The proposed optimizer was examined on medium- and large-scale IEEE test systems, including 30-bus, 118-bus, 300-bus and Algerian electricity grid DZA 114-bus (220/60 kV). The results of AEO algorithm are compared with well-known existing optimization techniques and results of comparison shown that the proposed algorithm performs better than other algorithms for all examined power systems. Consequently, we confirm the effectiveness of the introducing AEO algorithm to relieve the over losses problem, enhance power system performance, and meet solutions feasibility. One-way analysis of variance (ANOVA) has

been employed to evaluate the performance and consistency of the proposed AEO algorithm in solving ORPD problem.

Keywords: Artificial ecosystem optimization algorithm, optimal reactive power dispatch, real power loss, voltage deviation, voltage stability index, Large-scale test system.

List of Symbols	
P_{loss} / VD	The total power losses/voltage deviation
VSI	Voltage stability index
δ_{ij}	The voltage angle difference between i and bus j
θ_{ji} / V_{Gi}	The phase angle of term F_{ji} / voltage magnitude for generator at bus i
N_{PV}, N_{PQ}	The number of PV and PQ buses respectively
G_k	Conductance of k^{th} branch connected between bus i and j
V_i, V_j / $V_{L,N_{PQ}}$	Voltage magnitude of bus i and j/Voltage magnitude for load bus i
$\lvert Y_{ij} \rvert$ / S_i	The elements of bus admittance matrix/apparent power flow of branch i
$P_{D,i}$ / $Q_{D,i}$	The active/reactive, load consumption at bus i
P_{Gi} / Q_{Gi}	The active/reactive power generation at bus i
$P_{L,N_{PQ}}, Q_{L,N_{PQ}}$	The active and reactive power at each load bus
$V_i^{\max}, V_i^{\min}$	The maximum and minimum bus voltage magnitude at bus i
$Q_{Gi}^{\min}, Q_{Gi}^{\max}$	The minimum and maximum value of power generation at bus i
$T_k^{\max}$ / $T_k^{\min}$	The maximum/minimum tap ratio of k^{th} tap changing transformer
$Q_{Ci}^{\min}, Q_{Ci}^{\max}$	The minimum and maximum VAR injection limits of shunt capacitor
$S_i^{\max}$	The maximum apparent power flow limit of branch i
NB / NTL	The number of buses in the test system/number of transmission lines
NLB / NG	The number of load buses/The number of generators buses
NT / NC	The number of the transformer taps /number of shunt capacitor banks
λ_V, λ_Q, λ_I	The penalty factors
$X_i^{\lim}$	The limit value of the dependent variables $V_i^{\lim}$, $Q_i^{\lim}$, and $S_i^{\lim}$
$X_i^{\max}$ / $X_i^{\min}$	The maximum/minimum limit of state variables

1. Introduction

Electric Power System Operators (EPSO) are constantly seeking out new strategies to meet operational planning challenges for reducing power losses and ensuring continuity of services with less damages on electrical equipment's.[1][2] Until this date, optimal reactive power dispatch (ORPD) solution is the principal key for modern electric grid control, as well as, operation.

ORPD is a well-known complex combinatorial optimization problem with nonlinear characteristics. It is a sub-case of optimal power flow (OPF) problem. The principal mission of the ORPD solution is to determine steady condition operation parameters of all electrical equipment's of power system except the power of generators.[3] Efficient adjustment of control variables provide many benefits advantages to Electric Power System Operators (EPSO), such as help to convey energy to all existing loads in the network with a minimum losses of power while satisfying various physical and operational constraints imposed. Consequently, proper adjustment of control variables also helps all electric elements operate under service voltage.

In the ORPD, the active power of all generators available in the electric grid are fixed and known, except that of the slack-bus (reference). In the power flow study, total generation must be equal to the sum of all demand-loads connected and losses in the grid. Generator connected in the slack-bus balances the active power and reactive power flow in the whole of grid. The ORPD aims to find the set of optimal solutions of controlled variables by which the solutions found correspond to a minimum value of the selected objective function (power losses, or voltage deviation, or voltage stability index), while satisfying various equality and inequality constraints. The control variables consists of generator voltages as continuous variables, tap position of tap-changing transformers, and required number of shunt capacitors as discrete variables. The signification or the physic sense of equality-constraints is met by load flow analysis that reflects balance between supply and demand, whereas inequality-constraints are reflects the system operational and the security limits in the power system.

In the last decade, considerable complex research works have simulated using numerous nature-inspired optimization algorithms. These algorithms are inspired from evolution, swarm, biology and physics. Meta-heuristic algorithms can efficiently solve non-convex problem, non-differentiable objective-functions, and non-linear problems with mixed variables [4]. These solvers have ability to provide near-global solutions and have the capability to escape local ones, avoiding in premature convergence. Many meta-heuristic optimization techniques have been implemented to cope with ORPD problems. Thanh Long Duong *et al*. [5] presented a stochastic fractal search (SFS) method to solve optimal reactive power flow on the small-sized and medium test systems, while modified stochastic fractal search (MSFS) algorithm for ORPD was proposed by Thang Trung Nguyen *et al*. [6]. In addition, an improved gravitational search algorithm (GSA) associated with conditional

selection strategies (CSS) as novel constraints-handling method (GSA-CSS)for providing precise solutions to the ORPD problems [7], However, applied only on the medium-sized test systems and the reactive power of generators of IEEE 57-bus was enlarged to guarantee the feasibility of solutions. Also, the results obtained not compared with those reported works in the literature. Gaussian bare-bones teaching–learning-based optimization (GBTLBO) algorithm along with its modified version (MGBTLBO) for the ORPD problem with discrete and continuous control variables in the standard IEEE power systems was proposed in [8]. A hybrid technique named Gaussian bare-bones water cycle algorithm (GBWCA) [9] to solve ORPD problem was proposed. It has been applied on the medium-sized test systems IEEE 30-bus and IEEE 118-bus. Simulation shows that the results are encouraging. Ehsan Naderi et al. [10] proposed a novel fuzzy adaptive heterogeneous comprehensive-learning of PSO to deal with different versions of ORPD problem. It applied it on the large-scale test systems. Souhil *et al*. [11,12] proposed ant lion optimizer (ALO) and it version multi-objective (MOALO) algorithm to solve large scale power systems with discrete and continuous control variables. The experimental results show efficiency of algorithms with the feasibility of solutions. Also in [13] Souhil *et al*. proposed artificial bee colony algorithm to deal with discrete ORPD problem. Moth flame optimization (MFO) algorithm [14], and grey wolf optimizer (GWO) [15] were proposed for solving single objective ORPD problems. Again, however, the studies are limited on the medium test systems as IEEE 30-bus and IEEE 118-bus and only one objective function. Furthermore, a review study on meta-heuristic techniques applied to the ORPD field is presented in [16,17] and the statistics of publication per year as per web of knowledge since last 25 years can be found in [18]. However, these algorithms potentially suffer from few disadvantages or limitations such as the susceptibility of falling into local optima, and the difficulty of tuning the main intrinsic parameters. In addition, the application of these algorithms on large-scale test systems is uncommon. With the huge exploration of characteristics nature-inspired optimizer techniques, there is no universal technique has been capable to solve all optimization problems. Moreover, the variability of objective functions due to the use diverse functions to formulate ORPD problem. Thus, there is an opportunity to solve complex-problems by suggesting or exploring effective meta-heuristic techniques able deal different ORPD formulations is necessity.

In the previous contribution, the basic ALO algorithm has been employed to deal with different single aims ORPD formulations. [11] The findings proving outperform of ALO

solver over some recent published ones. In another contribution [12], we have also utilized MOALO algorithm to solve the same cases implying a conflicting objectives in large-scale test system, IEEE 300-bus. In this paper, a novel intelligent technique–called artificial ecosystem optimization (AEO) algorithm is presented in the field of ORPD solution. The principal-contributions of this paper are summarized below:

1- To the authors' best knowledge, this is the first attempt to apply artificial ecosystem optimization (AEO) algorithm to solve that ORPD problem effectively.

2- The exploration, exploitation and analysis is presented for a novel AEO algorithm to cope with the ORPD problem. More detail of exploration, exploitation and analysis concept can be found in [19]

3- Verification and validation of the performance of AEO computing heuristic is substantiated on three well-known IEEE test systems, 30-bus, 118-bus, 300-bus, and on the practical Algerian electricity grid DZA 114-bus.

4- Carrying out a comparative study between the proposed outcomes of AEO algorithm and implemented state of the art optimization algorithms on the ORPD solution in field.

Furthermore, the following points describe the main characteristics or major benefits of AEO technique, which definitely serve as motivational factors to choose this optimizer for dealing such optimization tasks.

1. It benefits from a well balance of exploration and exploitation phases [20] that assists this optimizer to escape local minima.
2. The exploration phase can be improved during consumption scheme using two strategies: (i) via updating solutions offered by the production process and (ii) an individual randomly selected having higher energy level.[21]
3. It has the same probability to choose between three types of consumers during consumption process, which might lead to bring an approximate mathematical modeling.

4. The decomposition process allows updating the coordinates of solutions based on the best solution achieved within population via key factors that improve the quality of solution significantly.[22]
5. It only requires two external parameters to adjust, such as population-size and maximum number of iterations, which makes it simple to implement and smooth execution.
6. The AEO algorithm has an excellent convergence capability to reach near optimal solution efficiently. The first online stochastic algorithms for the quantification problem with rigorous theoretical analysis are presented in [23].

The rest of the article is organized as follows: Section 2 covers the problem definition, objectives and mathematical formulation of ORPD problem. The description of proposed method is presented in Section-3. Section 4 introduces the experimental results, discussion along with comparison findings with some of newly meta-heuristic algorithms. Section 5 reveals statistical results and conclusion is given in Section-6.

2. Problem formulation

The mathematical formulation of the ORPD problem is amply described as objective functions and constraints, where these functions are minimized while fulfilling equality and inequality constraints. The problem is formulated as follows:

$$\text{Min} \quad \text{F} = Minimize \; F_{Obj}\left(x,u\right) \tag{1}$$

$$\text{Subject to:} \begin{cases} g\left(x,u\right)=0 \\ h\left(x,u\right)\le 0 \end{cases} \tag{2}$$

where $F_{F_{Obj}}\left(x,u\right)$ is the objective function, $g\left(x,\text{u}\right)$ equality constraints, $h\left(x,\text{u}\right)$ inequality constraints;

x : is the vector of dependent variables, consisting of load bus voltages, reactive power of generators, and transmission lines loading. Mathematically, it is written as follows:

$$x^{T}=\left[V_{L}...V_{L,N_{PQ}}\,,\,Q_{g,1}...Q_{g,N_{PV}}\,,S_{1}...S_{NTL}\right] \tag{3}$$

u: is the vector of control variables, comprising the mixed control variables involving voltages of the PV-bus as (continuous variables), transformer tap settings and switching shunt capacitor banks as (discrete variables). Hence, u is written as follows:

$$u^T = \left[\overbrace{V_{g,1}....V_{g,N_{PV}}}^{\text{continuous}} , \overbrace{T_1....T_{NT}, Q_{C1} ....., Q_{C,NC}}^{\text{Discrete}} \right] \tag{4}$$

In the present work, two different objective functions are considered:

- Minimization of total real power losses;
- Minimization of total voltage deviation (*TVD*); and
- Minimization of voltage stability index (*VSI*)

2.1 Objective functions

2.1.1 *Objective 1: minimization of total active power losses*

In general, the ORPD aims to minimize the total real power losses via an optimal adjustment to the control variables of the power system [24]. Mathematically, it is characterized as follows**:**

$$\mathrm{F}_1(x,\mathrm{u}) = \min P_{\mathrm{Loss}} = \sum_{k=1}^{NTL} G_k \times \left(V_i^{\,2} + V_j^{\,2} - 2 \times V_i \times V_j \times \cos\delta_{ij} \right) \tag{5}$$

2.1.2 *Objective 2: minimization of total voltage deviation (VD)*

This objective function is introduced for ensuring the security of electric power system. This case aimed to reduce the load-bus voltages gap resulting from specified value and those obtained from calculations.

$$\mathrm{F}_2(x,\mathrm{u}) = \min VD(x,\mathrm{u}) = Minimize \sum_{i=1}^{Npq} \left| V_i - 1.0 \right| \tag{6}$$

2.1.3 *Objective 3: Minimization of voltage stability index (VSI)*

Liberalization of energy market lead to increasing demand for electricity, which makes operation of an electric power grids become close to their stability limits. Therefore, the continuous monitoring and control of power system via voltage stability enhancement is necessity in order to get more information's on the voltage drops. The operating interval of index L was set in [0, 1] [25] The objective function to be minimized is defined as follow:

where L_j of the j^{th} bus is given by the following expression:

$$L_j = \left| 1 - \sum_{i=1}^{N_{PV}} F_{ji} \times \frac{V_i}{V_j} \angle \left\{ \theta_{ji} + \left(\delta_i - \delta_j \right) \right\} \right| \quad j = 1,2,...,N_{PQ} \tag{7}$$

with $F_{ji} = |F_{ji}| \angle \theta_{ji}$, $V_i = |V_i| \angle \delta_i$, $V_j = |V_j| \angle \delta_j$ $F_{ji} = -[Y_1]^{-1} \times [Y_2]$ (8)

Y_1, Y_2, Y_3, and Y_4 : are the sub-matrices of the system Y_{bus} obtained after rearranging the *PQ* and *PV*-bus bar parameters as shown in Eq. (9).

$$\begin{bmatrix} I_{PQ} \\ I_{PV} \end{bmatrix} = \begin{bmatrix} Y_1 & Y_2 \\ Y_3 & Y_4 \end{bmatrix} \times \begin{bmatrix} V_{PQ} \\ V_{PV} \end{bmatrix} \tag{9}$$

2.2 System-Constraints

2.2.1 *Equality constraints*: are the power flow equations which are given below:

$$\begin{cases} P_{Gi} - P_{di} - \sum_{j=1}^{NB} |V_i| \times |V_j| \times |Y_{ij}| \times \cos \times \left(\theta_{ij} - \delta_i + \delta_j \right) = 0 \\ Q_{Gi} - Q_{di} - \sum_{j=1}^{NB} |V_i| \times |V_j| \times |Y_{ij}| \times \sin \times \left(\theta_{ij} - \delta_i + \delta_j \right) = 0 \end{cases} \tag{10}$$

2.2.2 Inequality constraints represent the limits applied on the following variables.

$$\begin{cases} V_{g,i}^{\min} \le V_{g,i} \le V_{g,i}^{\max}, & \\ Q_{g,i}^{\min} \le Q_{g,i} \le Q_{g,i}^{\max}, & i = 1,2.....Ng \\ V_i^{\min} \le V_i \le V_i^{\max} & i \in NB \\ T_k^{\min} \le T_k \le T_k^{\max} & k \in NT \\ Q_{Ci}^{\min} \le Q_{Ci} \le Q_{Ci}^{\max} & i \in NC \\ S_l \le S_l^{\max} & l \in NTL \end{cases} \tag{11}$$

In this work, the concept of penalty functions is used, where only the violating variables such as (V_i, Q_G, and S_l) are added to the F_{obj} in order to discard any unfeasible solution obtained during the optimization process. Then, the modified objective function is written as follows:

$$F = F_{obj}(x, \mathrm{u}) + \lambda_V \times \sum_{i=1}^{N_{PQ}} \Delta V_i + \lambda_Q \times \sum_{i=1}^{NG} \Delta Q_i + \lambda_l \times \sum_{i=1}^{NTL} \Delta S_i \tag{12}$$

where λ_V, λ_Q, and λ_l are the penalty factors; X_i^{limit} is the limit value of each of the following variables: V_i, Q_i and S_i

$$\Delta X_i = \begin{cases} \left(X_i^{\min} - X_i\right)^2 & \text{if} \quad X_i < X_i^{\min} \\ \left(X_i - X_i^{\max}\right)^2 & \text{if} \quad X_i > X_i^{\max} \\ 0 & \text{if} \quad X_i^{\min} \le X_i < X_i^{\max} \end{cases} \tag{13}$$

3. Artificial Ecosystem Optimization (AEO) And Mathematical Formulation

Artificial Ecosystem Optimization (AEO) algorithm is a novel nature-inspired technique was first proposed by *Weiguo Zhao* et al., in [26] to efficiently tackle engineering optimization problems. An ecosystem is a group of living organisms such as animals, people, and plants live together in a particular area and it explains the correlation between them. Ecosystem is first divided to two parts: (i) living and (ii) non-living organisms. The living organisms include people, animals, plants, and bacteria and the non-living organisms include water, lawn, and sunlight. AEO is a population-based algorithm that mimics the behaviors of living organisms in nature, production, consumption, and decomposition processes on the surface of earth. The principal effort to maintain ecological equilibrium in an ecosystem is the flow of energy and the food resources. An ecosystem classifies the living elements into three distinct groups of organisms, namely, producers, consumers, and decomposers. The first group is the producer, which is the plants (An autotroph) since they produces its own energy through photosynthesis. The second is the consumer like animals, which depend on the other organisms which depend on one another either by its family or from the producer for gets energy. The third class of living organisms is the decomposers, which include most bacteria and fungi. Once an organism is died, the decomposers starts to break down the remain matter and converting them into a novel energy in form of water, minerals, and carbon dioxide. Then, these simple molecules serve as feeding source to the producers to again produce sugar and oxygen through photosynthesis and the process of cycle will be repeated.

The three kinds of living organism interact in many ways with each other in forming a food chain, which can guarantee a stable flow of energy within it. Some organisms feed from other ones proportional to the level of force and draws the path of energy in an ecosystem.

In an ecosystem, food web is made up of numerous interconnected and overlapping food chains, which describes a different ways of interconnections between them. These chains sorts the organisms based on their energy level. The producers are located usually at the up of the web food, whereas, the consumers are positioned at a higher level than what it consumes and they considered the most complicated one compared with others organisms. Figure 3 depicts

the path of energy in an ecosystem. From the Figure 3 it can be seen that organism with higher energy is assigned at the top of food grid whereas the lower energy organism is located at the bottom of the food grid.

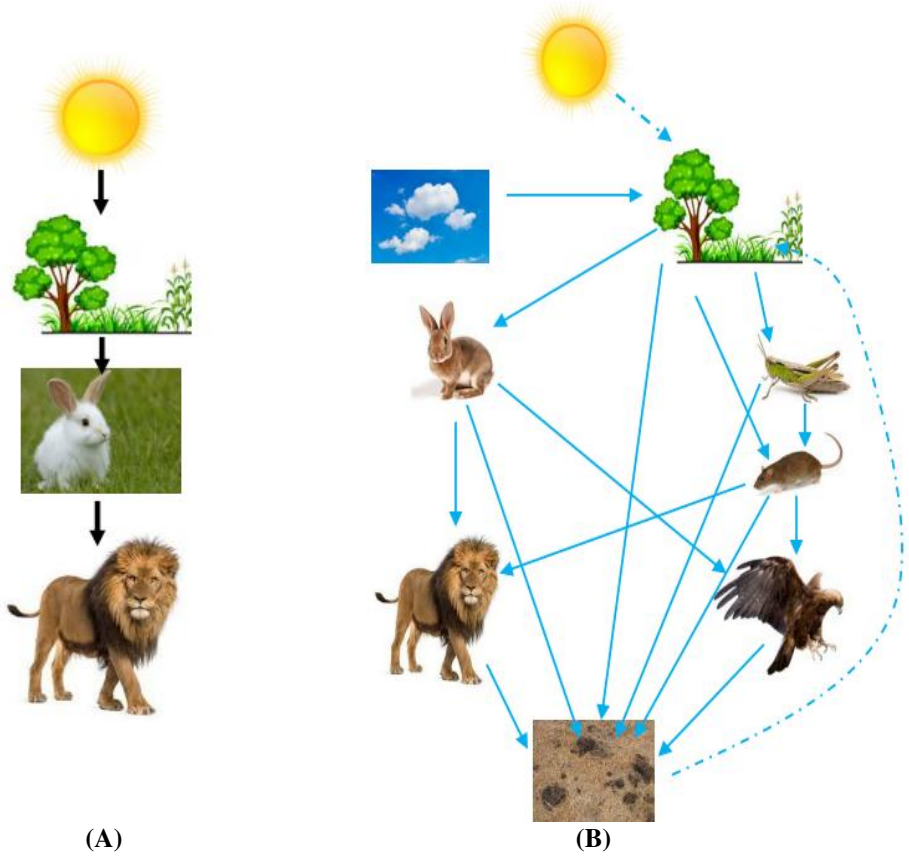

Fig. 3. Flow energy in an ecosystem; (a) food chain, (b) food web

As noted earlier, operation principal of AEO algorithm based on three phases, involving production, consumption, and decomposition. The first operator is the Producers. The first operator is carry to enhance the balance between the diversification and intensification abilities, while consumption was dedicated to exploitation process and the decomposition to ameliorate the exploitation process in this AEO. For each population, there is only one producer and one decomposer, while the remaining ones are the consumers. The fitness value is represented to the energy level of the each associated individual in a population. In other words, the individuals are sorted in a descending order according to their energy.

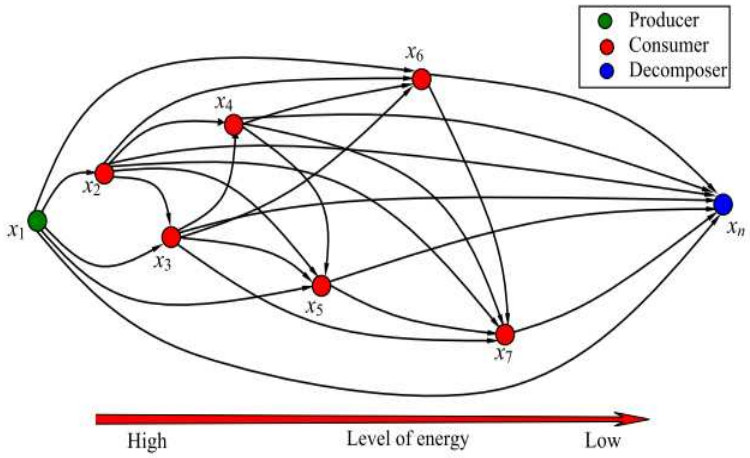

Fig. 4. A graph theory for an ecosystem based on the AEO.

4.2 Production

In this ecosystem, the candidates that have worst value of the function fitness are classified as the best ones, while the worst candidates correspond to the higher fitness value. The worst candidate x_1 associates with the highest energy level (Producer), whereas the best candidate x_n attached with lowest level of energy (Decomposer). The rest of candidates of the population are consumers: x_2, x_5 defined by herbivores, x_3, x_7 omnivores and x_4 with x_6 are carnivores.

The producer combines carbon dioxide, water, sunlight, and organic matter resulted from the decomposer to produce their food (energy) as sugar and oxygen. In this algorithm, the producer associated with lowest fitness value is updated according to their limits in search space. Based on this update, the other individuals in the population will try to update their positions. In AEO, the production operator generates a new individual to replace the old one between the better candidate (x_n) and a randomly generated candidate (X_{rand}) in the search space. Mathematically can be expressed as follows:

$$X_1(t+1) = (1-a)X_n(t) + a.X_{rand}(t) \tag{14}$$

$$a = \left(1 - \frac{iter}{max\_iter}\right) r_1 \tag{15}$$

$$X_{rand} = lb + r\left(ub - lb\right) \tag{16}$$

4.3 Consumption

Once the production operator is attained, the consumers start to perform the consumption operator in order to obtain food energy. In this phase, the consumers eat other consumer of a low energy or a producer or the both together. Afterwards, the Levy flight concept is utilized in an effort to improve the exploration patterns. The Levy flight usually mimics the real searching mechanism of animals. A consumption parameter treated by the Levy flight concept is defined as follows:

$$C = \frac{1}{2}\frac{v_1}{|v_2|} \tag{17}$$

$$v_1 \sim N\left(0, 1\right), \;\; v_2 \sim N\left(0, 1\right) \tag{18}$$

Where $N\left(0, 1\right)$ is a normal distribution of {mean= 0 and STD =1}. This consumption factor is mainly very helpful for each living consumers for gaining the food by utilizing the possible hunting techniques.

If a consumer is randomly picked as herbivore, it will eat only the producers. This behavior is expressed mathematically by Eq. (19):

$$X_i\left(t+1\right) = X_i\left(t\right) + C.\left(X_i\left(t\right) - X_1\left(t\right)\right), \quad i \in \left[2, ..., n\right] \tag{19}$$

In case of a consumer is picked as a carnivore, then it will eat only consumers having lower fitness value. This behavior can be represented by Eq. (20).

$$\begin{cases} X_i\left(t+1\right) = X_i\left(t\right) + C.\left(X_i\left(t\right) - X_j\left(t\right)\right), i \in \left[3, ..., n\right] \\ j = randi\left(\left[2i - 1\right]\right) \end{cases} \tag{20}$$

With the last case of consumption phase, when the consumer is considered as an omnivore, then it will be able to eat other consumers having higher energy level and producers too. This behavior is given by Eq. (21)

$$\begin{cases} X_i\left(t+1\right) = X_i\left(t\right) + C.\left(r_2\left(X_i\left(t\right) - X_j\left(t\right)\right)\right) + \left(1 - r_2\right)\left(X_i\left(t\right) - X_j\left(t\right)\right) \\ i \in \left[3, ..., n\right] \\ j = randi\left(\left[2i - 1\right]\right) \end{cases} \tag{21}$$

4.4 Decomposition

Decomposition parameter is more important for the AEO, which act after each death of any individual in the population to decay the residues of that individual. To gain an approximate mathematical model of this behavior, some parameters such as the decomposer factor D, weight variables e and h are considered.

4. To gain an approximate mathematical model of this behavior, some parameters such as the decomposer factor D, weight variables e and h are considered. Then, each individual X_i updates its coordinates based on the decomposer X_n and through predefined parameters: such as D, e, and h based on the following equations:

$$X_i(t+1) = X_n(t) + D.\left(e.X_n(t) - h.X_i(t)\right),\ i = 1,.....,n \tag{22}$$

$$D = 3u,\ u \sim N(0,1) \tag{23}$$

$$e = r_3.randi\left([12]-1\right) \tag{24}$$

$$h = 2.r_3 - 1 \tag{25}$$

The optimization process in AEO starts with a population of individuals in which randomly generated into research space, then at each iteration the first individual (producer) updates its coordinates according to the Eq. (14), while other candidates in the population will hence try to update their coordinates based on its own best consumer by using Eqs. (15), (16), and (17), except in the case of the individual having a highest fitness value, then the position of that individual will be updated by using Eq. (19). All aforementioned updates are repeated until a terminal criterion is satisfied. Finally, the optimal or near-optimal solution that corresponds to a best individual found so far is memorized.

Algorithm 1: Pseudo code of the proposed load scheduling optimization algorithm

Read input power system-data (line data + bus data) and set the control variable limits
Input= Setting variables: pops-ize, Max-iter, dim, define lb and ub
Generate initial population for an ecosystem X_i ; i.e., Initialize random values of position of populations i.e. for each individual in population is a randomly generating a string of real values within their control variable defined by vector *u.*
Evaluation: run power flow for every candidate solution and calculate selected objective function F_{Obj_i}
Select best candidate solution, F_{Best} and saved it; Find X_{Best} from $PopF_t$,i.e., parameters of control variables correspond to the best candidate solution F_{Best}
    for Iter = 1 to Max-Iter **do**
    a (linearly decreased from 1 to 0), and Parameters: param.u, param**.v**, and param.**C**
    Update the Position X1, according to Equation **(14)**
    for i = 3 to PopSize **do**
        if r < 1/3 or **if** 1/3 < r <2/3
        Update the Position Xi, according to Equation**s** (19)–(21)
        end if
    Evaluate the *ObjFun* for eah Xi according to Equation (1)
      if $ObjF_i \leq ObjF$ (i − 1) **then**
       replace the previous Position with the new one
      end if
    Find the BestOne so far
    Assign a new position by using Equation (22)
    end for
    for i = 1 to PopSize **do**
     Evaluate the *ObjFun* for eah Xi according to Equation (1)
      if $ObjF_i \leq ObjF$ (i − 1) **then**
          replace the previous Position with the new one
      end if
     Find the best one found so far
    end for
    end for
    Select the best position (solution) achieved so far and memorize it
end for
Return optimum solution (X_{best}) and display results of: PLoss/VD/VSI, *Vg*, Tap, and Q_{Ci}

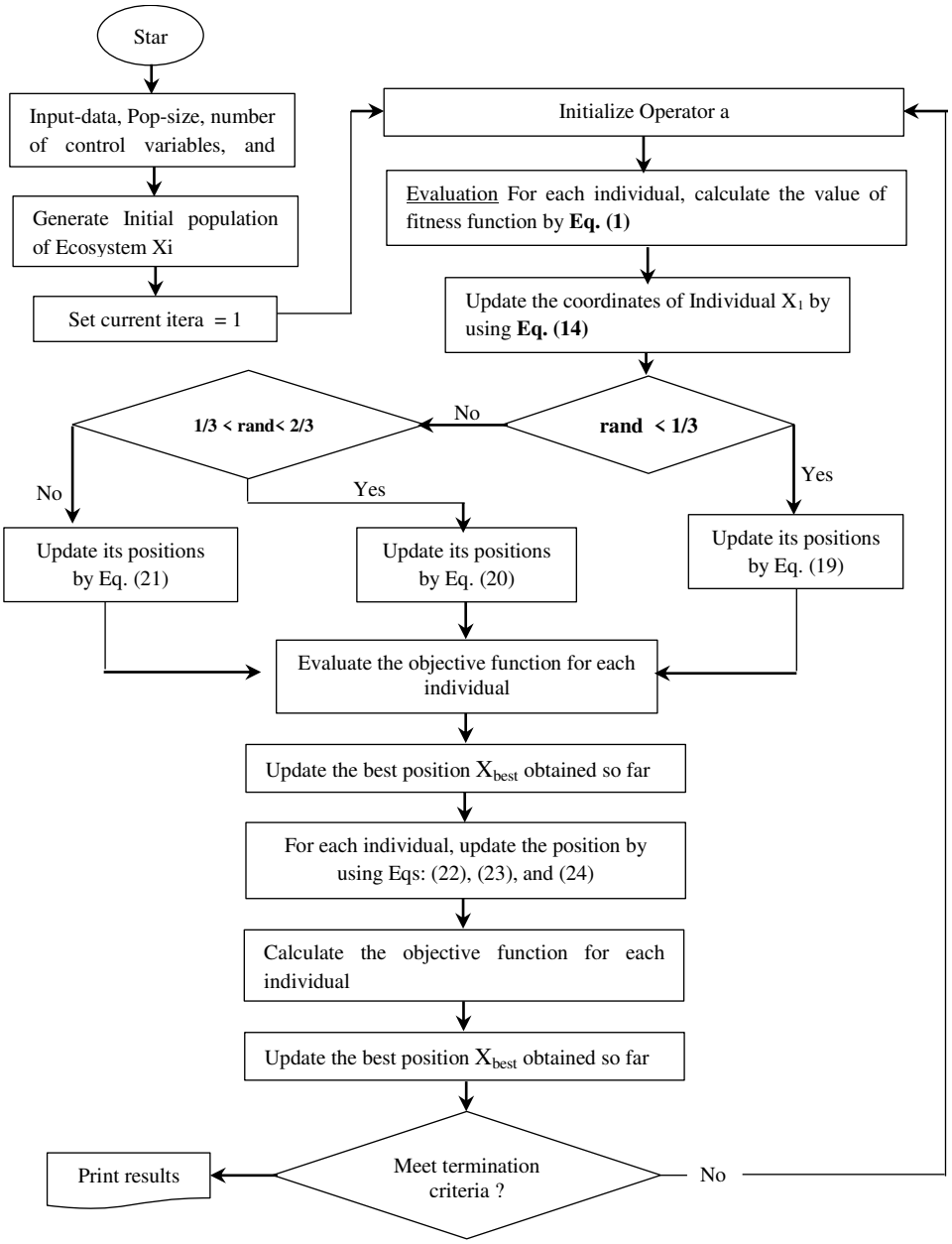

Fig. 5. Flowchart of AEO algorithm

The Pseudo-code of the proposed ORPD optimization algorithm is described in Algorithm 1**.** The Figure 5 shows the flowchart of proposed AEO algorithm.

5. Numerical Result and Discussion

To check the capability and robustness of the proposed AEO in solving three single ORPD formulations, the optimizer is executed on the IEEE 30-bus, IEEE 118-bus and IEEE 300-bus test systems as well as on the Algerian electricity grid DZA 114-bus. Furthermore, to validate the AEO algorithm, the well-known recently contributions published by ASOC are considered as competitors to solve ORPD cases. The algorithm was implemented in the MATLAB

Platform 7.10 and the simulation conducted on Laptop with a 1.90 GHz processor and 4 GB RAM. An empirical study was conducted to select the population size, i.e., we study the effect of population size on the performance of the AEO technique, in which 30 trial runs has been performed under different of population sizes like 20, 30, 40, and 70. The results of this study not introduced, but we only indicate that 30 individuals of population give best results for all case studies. For that reason, in all simulation cases, population size is specified as 30 individuals and maximum number of iteration is fixed 100 for IEEE 30-bus, 200 for DZA 114-bus, IEEE 118-bus and IEEE 300-bus test systems. For the purpose of comparison, in all simulation cases, we considered all control variables as continuous except those of Algerian power system DZA 114-bus. The number of hard variables and initial conditions were taken from [16,17].

Table 1. Description of all test-systems characteristics used in this article

Description	**IEEE 30-bus**	**IEEE 118-bus**	**IEEE 300-bus**	**DZA 114-bus**
Buses, N_B	30	118	300	114
Generators, N_G	6	54	69	15
Transformers, N_T	4	9	107	16
Shunts, N_Q	9	14	14	7
Branches, N_E	41	186	411	175
Control variables	19	77	190	38
Discrete variables	6	21	121	23
Base case for P_{Loss}, p.u.	5.880	132.863	408.316	67.447
Base case for VD, p.u.	1.4942	1.43933	5.4286	3.82
Base case for L-index	0.1798	0.0694	0.4135	0.3421

Table 2. Control variables settings for all power systems

Test system	**Variables**	**Lowe**	**Upper**	**Step**
IEEE 30-bus [11]	V_{PV} and V_{PQ}	0.95	1.1	Continuous
	T	0.9	1.1	
	Q_{shunt} (9)	0	5	
IEEE 118-bus	V_{PV} and V_{PQ}	0.95	1.05	Continuous
	T	0.9	1.1	
	Q_{shunt} (14)	See in [15]		
IEEE 300-bus [27]	V_{PV} and V_{PQ}	0.9	1.1	Continuous
	T	0.9	1.1	
	Q_{shunt}	See in [28]		
DZA 114-bus	V_{PV} and V_{PQ}	0.9	1.1	Continuous
	T	0.9	1.1	0.01
	Q_{shunt}	See in [29]		Discrete

5.1 IEEE 30-bus test system [9][30]

This test system has 6 generators (PV buses) at buses 1, 2, 5, 8, 11, 13 while the rest are the load buses (PQ buses), 4 Transformers with off nominal tap ratio at the branches 11, 12, 15, and 36, as well as 9 shunt compensators at bus bars 10, 12, 15, 17, 20, 21, 23, 24, and 29 taken from [31]. The load demand is (2.834+j 1.262) p.u; its full data is given in [32]. In IEEE 30-bus test system, the upper and lower voltages bounds of all buses are chosen to be 1.1 p.u. and 0.95 p.u., respectively. The limits for other decision variables are taken from [5][33].

In this part, the adopted objective function is the real power loss minimization by means of the AEO, ALO, and NBA algorithms. Fig. 6 shows the convergence curves of the considered optimizers and, as noticeably, the AEO algorithm converges to high quality solutions in the first quarter of iterations. Based on the convergence plot presented in Fig. 6, it can be seen that AEO algorithm achieve the global optimal power losses in only 35^{th} iteration.

In addition, it can be seen that the AEO technique outperforms the NBA and ALO methods in terms of convergence characteristic as well as solution merit. The best settings of the control variables obtained via the implemented techniques AEO, NBA, and ALO are reported in Table 3. In the 30 independent runs performed, proposed AEO found the best solution. It can be seen that the real power loss achieved via AEO, NBA, and ALO algorithms are is 4.5262 MW, 4.5529 MW and 4.5919 MW, respectively. Fig. 7 illustrates the performance of AEO for 30 independent run of executions. It observed that the best and worst solutions are very close, with a difference of 0.3%. Noticeably, it was explored that a number of optimizers published seem to have violated the feasibility boundaries, rendering the solutions infeasible.

Compared recalculated results with obtained ones provided in Table 3, It clearly appears that all of implemented algorithms such as ALO, NBA, and proposed AEO gives exact values and insure the feasibility of solutions by keeping all state variables within the specified limits. The voltage profile at load buses-(PQ buses) for IEEE 30-bus is illustrated in Fig. 8.

Table 3. Solution of minimum power losses (MP) for IEEE 30-bus test system

Control variables	**FA** [30]	**DE** [24]	**QOTLB** [34]	**TLBO** [34]	**BBO** [35]	**ALO** [33]	**GSA** [30]	**MFO** [14]	**NBA**	**ALO**	**AEO**
Generator Voltage (p.u)											
$\mathbf{V_1}$	1.1000	1.1000	1.1000	1.1000	1.1000	1.1000	1.0999	1.1	1.1	1.1000	1.1000
$\mathbf{V_2}$	1.0644	1.0931	1.0942	1.0936	1.0944	1.0953	1.0743	1.0943	1.0951	1.0953	1.0944
$\mathbf{V_5}$	1.0745	1.0736	1.0745	1.0738	1.0749	1.0767	1.0749	1.0747	1.0775	1.0764	1.0751
$\mathbf{V_8}$	1.0869	1.0756	1.0765	1.0753	1.0768	1.0788	1.0768	1.0766	1.0792	1.0787	1.0770
$\mathbf{V_{11}}$	1.0916	1.1000	1.1000	1.0999	1.0999	1.1000	1.0999	1.1	1.0960	1.0916	1.1000
$\mathbf{V_{13}}$	1.0999	1.1000	1.0999	1.1000	1.0999	1.1000	1.0999	1.1	1.0998	1.0862	1.1000
Tap ratio (p.u)											
$\mathbf{T_{11}}$	1.00	1.0465	1.0664	1.0251	1.0435	1.01	1.00	1.0433	1.0313	1.0333	1.0392
$\mathbf{T_{12}}$	0.94	0.9097	0.9000	0.9439	0.9011	0.99	0.93	0.9	0.9424	1.0004	0.9000
$\mathbf{T_{15}}$	1.00	0.9867	0.9949	0.9992	0.9824	1.02	0.98	0.9791	1.0009	1.0361	0.9729
$\mathbf{T_{36}}$	0.97	0.9689	0.9714	0.9732	0.9691	1.000	0.97	0.9647	0.9854	0.9976	0.9632
Capacitor Banks (MVAR)											
$\mathbf{Q_{C\text{-}10}}$	3	5.0000	5.0000	5.0000	4.9998	4	3.7	5	4.2055	4.9477	4.9948
$\mathbf{Q_{C\text{-}12}}$	4	5.0000	5.0000	5.0000	4.987	2	4.3	5	5	4.8343	4.9963
$\mathbf{Q_{C\text{-}15}}$	3.3	5.0000	5.0000	5.0000	4.9906	4	3.7	4.8055	3.3446	4.5170	4.8409
$\mathbf{Q_{C\text{-}17}}$	3.5	5.0000	5.0000	5.0000	4.997	3	2.2	5	5	4.7030	4.9985
$\mathbf{Q_{C\text{-}20}}$	3.9	4.4060	4.45	4.57	4.9901	2	3.1	4.0623	4.3974	3.5384	4.2895
$\mathbf{Q_{C\text{-}21}}$	3.2	5.0000	5.00	5.00	4.9946	4	3.9	5	4.9844	4.5841	5
$\mathbf{Q_{C\text{-}23}}$	1.3	2.8004	2.83	2.86	3.8753	3	4.2	2.5193	4.8984	4.8054	2.6464
$\mathbf{Q_{C\text{-}24}}$	3.5	5.0000	5.00	5.00	4.9867	5	4.4	5	3.7526	4.9123	4.9998
$\mathbf{Q_{C\text{-}29}}$	1.42	2.5979	2.56	2.58	2.9098	5	2	2.1925	2.8649	2.8453	2.2293
$\mathbf{P_{Loss}}$ (MW)	**4.5691**	**4.5550**	**4.5594**	**4.5629**	**4.5511**	**4.59**	**4.54**	**4.534**	**4.55293**	**4.5919**	**4.5262**
P_{Loss} Calculated		**4.532**	**4.535**	**4.538**	**4.532**	**4.590**	**4.952**[a]	**4.527**	**4.553**	**4.592**	**4.526**
VD	1.7752	1.9589	1.9057	1.8760	NA	NA	1.92	NA	1.5270	1.2210	**1.83**
L-index	NA	0.5513	0.1273	0.1278	NA	0.1307	NA	NA	0.1285	0.1323	**0.1250**
CPU (s)	NA	NA	NA	NA	110	98	NA	NA	65	85	**116**

Bold results are the Best one achieved by AEO

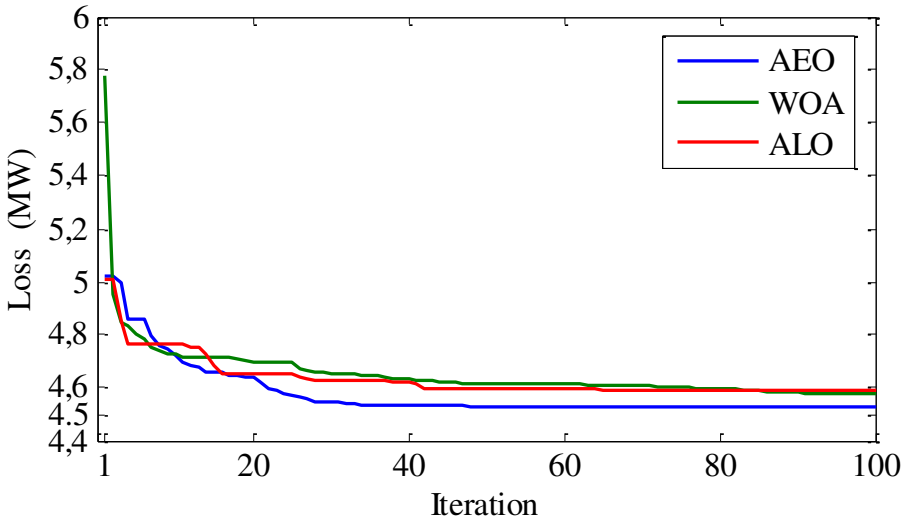

Fig. 6. Convergence characteristic of IEEE 30-bus system for P_{Loss} minimization

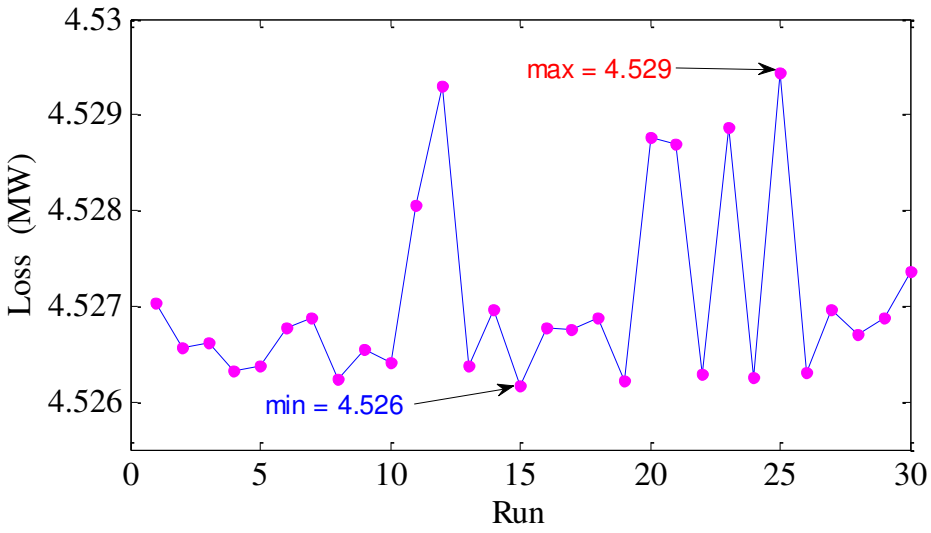

Fig. 7. Performance of 30 individuals for 30 independent execution runs

5.1.1 Results of IEEE 30-bus when increasing iterations number to 1k, 10k and 50 k

The minimum losses P_{loss} are presented in Table 3.1. It can be seen that there is no a difference between NBA and AEO algorithms and slight difference with ALO algorithm. We can conclude that consistency of NBA is very well to find near-optimal solution and competitor to the proposed AEO algorithm in the medium-sized test system.

Table 3.1 Results of IEEE 30-bus vs. iteration numbers

Algorithms	**NBA**			**ALO**			**AEO**		
Iteration	1k	10k	50k	1k	10k	50k	1k	10k	50k
P_{Loss} (MW)	4.5267	4.5261	4.5261	4.5736	4.5621	4.5516	4.5261	4.5261	4.5261
VD (p.u.)	1.575	1.5519	1.5519	1.292	1.3359	1.415	1.5519	1.5519	1.5519
L-index	0.1247	0.1249	0.1249	0.1283	0.1278	0.1264	0.1249	0.1249	0.1249

5.2 *IEEE 118-bus test system* [32]

IEEE 118-bus test system consist of one hundred eighty-six branches, fifty four generators, sixty four load buses, nine branches under load tap-changing transformers and fourteen reactive power sources. The load demand is (42.42+j 14.38) p.u., under base power of 100 MW. The complete data can be found in [27]. The minimum and maximum limits of variables can be found in [14]. Two cases are considered as follows:

Case 1: minimization of P_{Loss}.

Case 2: minimization of *VD*.

Case 1: Minimization of active power losses

Table 4 shows the obtained findings of active power losses minimization case and the corresponding control variables settings for IEEE 118 bus test system. The results confirm that the proposed AEO is able to provide the best result than other optimization techniques listed, both with respect of the solution quality and validity. From the results of this case, AEO reduces the power losses to 115.302 MW, i.e., 3.78 % less than ALO, 6.14 % less than NBA 0.97 % less than MFO, 4.63 % less than GWO, 10.13 % less than OGSA, 13.57 % less than PSO, 10.81 % less than GSA. These significant values reflect substantial improvement in the achieved findings. Fig. 8 shows the bus voltage profiles for the best obtained solutions. Remarkably, the magnitude of voltages is exactly inside the defined range which affirm the feasibility of solutions the AEO algorithm. Fig. 10 discloses the performance of AEO for 30 independent execution runs. It observed that the best and worst results are 115.3027 MW and 116.938 MW, respectively in which difference between them is no longer than 1.64 MW. The convergence curves of real power loss for IEEE 118-bus system for three implemented algorithms AEO, NBA and ALO is presented in Fig. 9. According to the Fig. 9, it is clearly that proposed algorithm find the optimal real power loss after 80th iteration. Moreover, it is clearly that the proposed AEO takes lesser execution time as compared to CPVEIHBMO, GSA, PSO, OGSA, GWO, and MFO. However, ALO and NBA solvers require less time to complete the simulation.

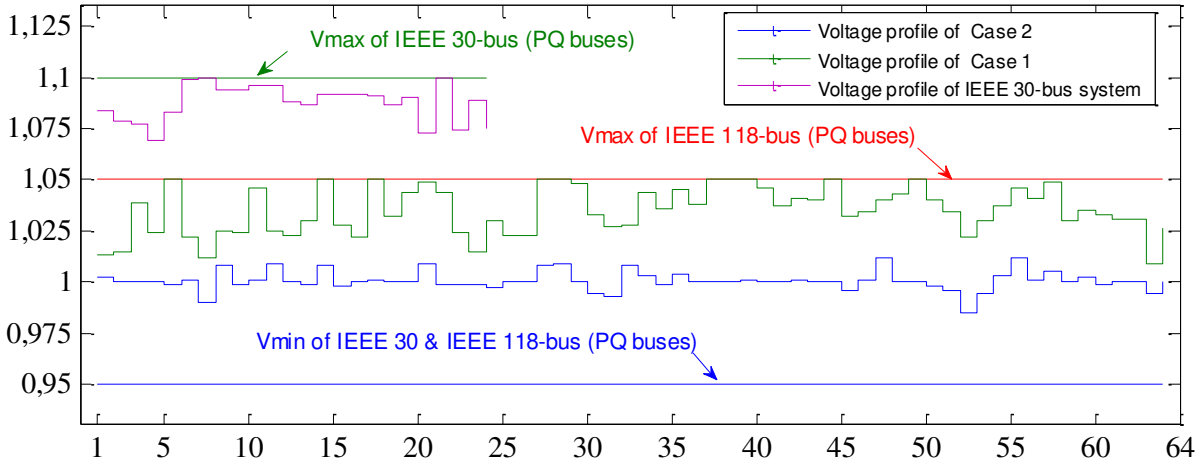

Fig. 8. Voltage profile at load buses-(PQ buses) for IEEE 30 and 118-bus power systems

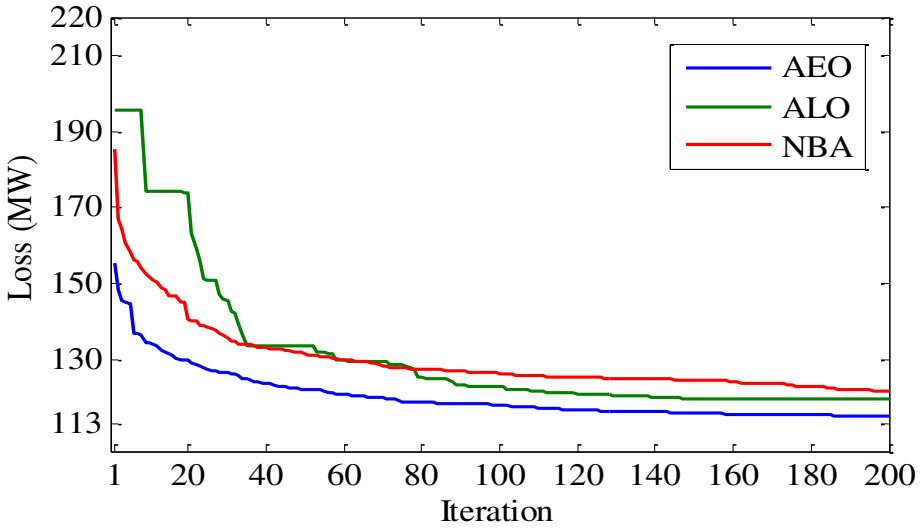

Fig. 9. Comparative convergence curves for P_{Loss} minimization of the 118-bus

Table 4. Solution of minimum power losses for power system 118-bus system

Cont varia	CPVEIH BMO	GSA [32]	PSO	OGSA [36]	GWO [15]	MFO [14]	NBA	ALO	AEO
Generator Voltage (p.u)									
V_1	0.9926	0.9600	1.0332	1.035	1.0204	1.0173	1.0429	1.0242	1.0090
V_4	1.0108	0.9620	1.055	1.0554	1.0257	1.0402	1.0415	1.0439	1.0388
V_6	1.0037	0.9729	0.9754	1.0301	1.0208	1.0292	1.0495	1.0349	1.0248
V_8	0.9976	1.0570	0.9669	1.0175	1.0419	1.0600	1.0457	1.0269	1.0366
V_{10}	1.0215	1.0885	0.9811	1.025	1.0413	1.0374	1.0313	1.0608	1.0419
V_{12}	1.0093	0.9630	1.0092	1.041	1.0232	1.0250	1.0429	1.0348	1.0241
V_{15}	1.0075	1.0127	0.9787	0.9973	1.0207	1.0268	1.0317	1.0363	1.0313
V_{18}	1.0259	1.0069	1.0799	1.0047	1.0270	1.0298	1.0406	1.0530	1.0363
V_{19}	0.9943	1.0003	1.0805	0.9899	1.0204	1.0275	1.0337	1.0402	1.0338
V_{24}	1.0179	1.0105	1.0286	1.0287	1.0137	1.0483	1.0388	1.0500	1.0469
V_{25}	1.0177	1.0102	1.0307	1.06	1.0270	1.0600	1.0453	1.0664	1.0768
V_{26}	0.9990	1.0401	0.9877	1.0855	1.0386	1.0600	1.033	1.0465	1.0858
V_{27}	1.0084	0.9809	1.0157	1.0081	1.0188	1.0267	1.0298	1.0365	1.0403
V_{31}	0.9838	0.9500	0.9615	0.9948	1.0138	1.0101	1.0408	1.0352	1.0229
V_{32}	0.9827	0.9552	0.9851	0.9993	1.0135	1.0226	1.0479	1.0302	1.0325
V_{34}	1.0065	0.9910	1.0157	0.9958	1.0261	1.0556	1.0284	1.0409	1.0453
V_{36}	1.0190	1.0091	1.0849	0.9835	1.0261	1.0548	1.0336	1.0374	1.0442
V_{40}	1.0267	0.9505	0.983	0.9981	1.0125	1.0419	1.0239	1.0215	1.0210
V_{42}	0.9865	0.9500	1.0516	1.0068	1.0233	1.0429	1.0322	1.0147	1.0228
V_{46}	1.0084	0.9814	0.9754	1.0355	1.0272	1.0450	1.042	1.0367	1.0419
V_{49}	1.0035	1.0444	0.9838	1.0333	1.0401	1.0589	1.0413	1.0582	1.0567
V_{54}	0.9806	1.0379	0.9637	0.9911	1.0230	1.0284	1.046	1.0179	1.0431
V_{55}	0.9969	0.9907	0.9716	0.9914	1.0221	1.0289	1.0438	1.0111	1.0459
V_{56}	0.9881	1.0333	1.025	0.992	1.0226	1.0283	1.0501	1.0147	1.0456
V_{59}	1.0197	1.0099	1.0003	0.9909	1.0379	1.0512	1.0466	1.0494	1.0548
V_{61}	0.9956	1.0925	1.0771	1.0747	1.0241	1.0534	1.0467	1.0526	1.0459
V_{62}	1.0064	1.0393	1.048	1.0753	1.0199	1.0506	1.0446	1.0505	1.0474
V_{65}	0.9883	0.9998	0.9684	0.9814	1.0465	1.0596	1.0529	1.0436	1.0532
V_{66}	1.0101	1.0355	0.9648	1.0487	1.0378	1.0600	1.0389	1.0669	1.0626
V_{69}	0.9931	1.1000	0.9574	1.049	1.0501	1.0600	1.0417	1.0568	1.0717

V_{70}	1.0127	1.0992	0.9765	1.0395	1.0243	1.0600	1.0338	1.0185	1.0462
V_{72}	1.0145	1.0014	1.0243	0.99	1.0187	1.0526	1.049	1.0462	1.0480
V_{73}	1.0174	1.0111	0.9651	1.0547	1.0397	1.0600	1.0467	1.0090	1.0437
V_{74}	1.0025	1.0476	1.0733	1.0167	1.0170	1.0600	1.032	1.0230	1.0395
V_{76}	0.9842	1.0211	1.0302	0.9972	1.0080	1.0390	1.0316	1.0272	1.0269
V_{77}	0.9914	1.0187	1.0275	1.0071	1.0192	1.0502	1.0407	1.0316	1.0465
V_{80}	1.0257	1.0462	0.9857	1.0066	1.0329	1.0600	1.0413	1.0372	1.0535
V_{85}	0.9876	1.0491	0.9836	0.9893	1.0224	1.0600	1.0421	1.0421	1.0499
V_{87}	1.0213	1.0426	1.0882	0.9693	1.0361	1.0599	1.0519	0.9965	1.0555
V_{89}	1.0069	1.0955	0.9895	1.0527	1.0558	1.0600	1.0427	1.0657	1.0679
V_{90}	1.0298	1.0417	0.9905	1.029	1.0290	1.0431	1.0385	1.0289	1.0378
V_{91}	0.9839	1.0032	1.0288	1.0297	1.0127	1.0496	1.0266	1.0353	1.0341
V_{92}	1.0021	1.0927	0.976	1.0353	1.0360	1.0600	1.0369	1.0576	1.0552
V_{99}	0.9853	1.0433	1.088	1.0395	1.0297	1.0551	1.0262	1.0453	1.0454
V_{100}	1.0281	1.0786	0.9617	1.0275	1.0360	1.0584	1.0445	1.0507	1.0523
V_{103}	0.9802	1.0266	0.9611	1.0158	1.0232	1.0442	1.0404	1.0425	1.0461
V_{104}	1.0187	0.9808	1.0125	1.0165	1.0180	1.0333	1.0314	1.0430	1.0467
V_{105}	1.0209	1.0163	1.0684	1.0197	1.0176	1.0281	1.0345	1.0459	1.0389
V_{107}	1.0234	0.9987	0.9769	1.0408	1.0201	1.0161	1.0517	1.0848	1.0271
V_{110}	0.9842	1.0218	1.0414	1.0288	1.0207	1.0215	1.0313	1.0366	1.0326
V_{111}	1.0000	0.9852	0.979	1.0194	1.0261	1.0280	1.0419	1.0591	1.0418
V_{112}	0.9930	0.9500	0.9764	1.0132	1.0066	1.0042	1.0311	1.0185	1.0190
V_{113}	1.0200	0.9764	0.9721	1.0386	1.0251	1.0350	1.0476	1.0398	1.0410
V_{116}	1.0016	1.0372	1.033	0.9724	1.0342	1.0484	1.0372	1.0261	1.0522
Tap ratio setting of transformers									
$\mathbf{T_8}$	1.0255	1.0659	1.0045	0.9568	1.0208	1.0136	1.032	0.9700	0.9933
$\mathbf{T_{32}}$	0.9891	0.9534	1.0609	1.0409	1.0279	1.1000	0.99874	1.0217	1.0999
$\mathbf{T_{36}}$	0.9932	0.9328	1.0008	0.9963	1.0323	1.0038	0.99845	1.0035	0.9896
$\mathbf{T_{51}}$	0.9873	1.0884	1.0093	0.9775	1.0209	0.9826	1.0059	0.9642	0.9762
$\mathbf{T_{93}}$	0.9868	1.0579	0.9922	0.956	1.0091	0.9843	0.97775	0.9696	0.9641
$\mathbf{T_{95}}$	1.0235	0.9493	1.0074	0.9956	1.0366	1.0139	0.99487	1.0059	1.0145
$\mathbf{T_{102}}$	1.0090	0.9975	1.0611	0.9882	1.0301	1.1000	1.0052	1.0204	0.9569
$\mathbf{T_{107}}$	1.0075	0.9887	0.9307	0.9251	1.0234	1.1000	0.99449	0.9827	0.9464
$\mathbf{T_{127}}$	0.9872	0.9801	0.9578	1.0661	1.0211	0.9683	1.0055	1.0440	0.9792
Reactive power of shunt resources (MVAR)									
$\mathbf{Q_{C\text{-}5}}$	0	0	0	−33.19	−39.76	0	−17.747	−3.2410	−8.9587
$\mathbf{Q_{C\text{-}34}}$	6.0111	7.4600	11.714	4.8	13.7900	0	1.8726	1.7198	6.4884
$\mathbf{Q_{C\text{-}37}}$	0	0	0	−24.9	−24.73	−0.03126	−5.5757	−12.8228	−8.8591
$\mathbf{Q_{C\text{-}44}}$	6.0057	6.0700	9.8932	328	9.9571	10	0	0.4357	5.6581
$\mathbf{Q_{C\text{-}45}}$	3.0001	3.3300	9.4169	3.83	9.8678	0	8.5929	1.4848	7.0815
$\mathbf{Q_{C\text{-}46}}$	5.9838	6.5100	2.6719	5.45	9.9186	0	5.6952	3.2751	4.9572
$\mathbf{Q_{C\text{-}48}}$	3.9920	4.4700	2.8546	1.81	14.8900	0.00084	7.3115	6.3305	7.0284
$\mathbf{Q_{C\text{-}74}}$	7.9862	9.7200	0.5471	5.09	11.9720	0.22054	5.0436	1.1433	1.8367
$\mathbf{Q_{C\text{-}79}}$	13.9892	14.2500	14.853	11.04	19.6490	20	15.242	10.8565	16.778
$\mathbf{Q_{C\text{-}82}}$	17.9920	17.4900	19.427	9.65	19.8900	0	16.258	1.1730	14.582
$\mathbf{Q_{C\text{-}83}}$	4.0009	4.2800	6.9824	2.63	9.9515	10	6.6489	1.4741	4.9715
$\mathbf{Q_{C\text{-}105}}$	10.9825	12.0400	9.0291	4.42	19.9680	0	5.6212	16.9174	0.0077
$\mathbf{Q_{C\text{-}107}}$	2.0251	2.2600	4.9926	0.85	5.9136	6	3.8228	3.5582	2.7109
$\mathbf{Q_{C\text{-}110}}$	2.0272	2.9400	2.2086	1.44	5.8834	6	3.0696	0.3696	2.3012
$\mathbf{P_{loss}}$	124.098	127.76	130.96	126.99	120.65	116.4254	122. 391	119.6645	**115.3027**
L-max	NA	NA	NA	NA	NA	NA	0.06540	0.06466	**0.06373**
CPU(s)	1053	1198	1472	1101.2	1372	1419	417	568	**886**

-Bold results denote best results

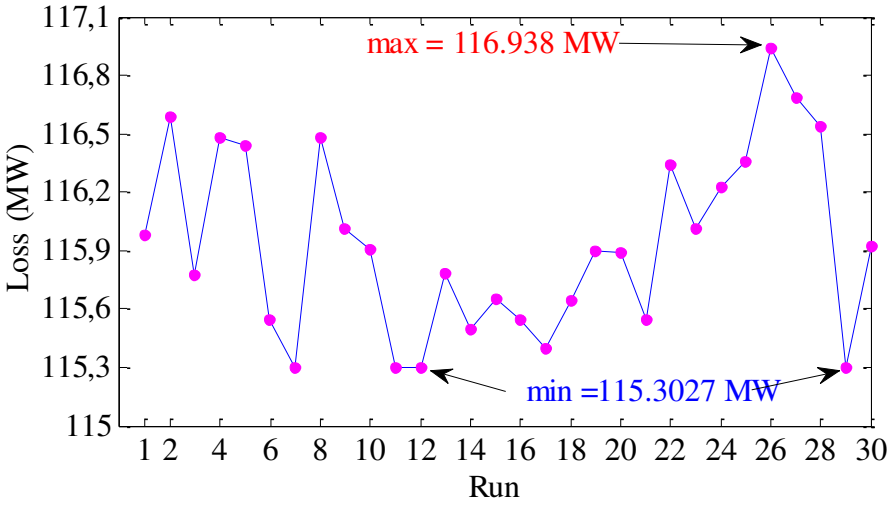

Fig. 10. Performance of 30 individuals for 30 independent execution runs

Table 5 reveals comparison results of AEO and a number of optimizers reported in the literature and the corresponding percentages of power losses reduction. The greatest reduction is achieved by AEO algorithm which is 13.21 % with regard to the base case and better than those reported by other algorithms. Thus, simulation results confirm that AEO algorithm can define the optimal solution or near-optimal solution, even with large-scale test system.

5.2.1 Results of IEEE 118-bus when increasing iterations number to 1k, 10k and 50 k

Table 4.1 Results of IEEE 118-bus vs. iteration numbers

Algorithms	**NBA**			**ALO**			**AEO**		
Iteration	1k	10k	50k	1k	10k	50k	1k	10k	50k
$\mathbf{P_{Loss}}$ (MW)	116.176	114.917	114.210	115.736	114.540	114.497	114.246	114.20	**114.177**
VD	3.188	3.423	3.624	3.4459	3.5819	3.6029	6.564	6.6691	**6.6340**
L-index	0.0644	0.0640	0.06395	0.06407	0.06938	0.06375	0.0637	0.0635	**0.06357**

Table 4.1 reports new simulation results when increasing the iteration numbers to 1k, 10k and 50k for IEEE 118-bus test system, in which we can observed clearly that also even with large number of iteration of the proposed AEO algorithm keep its consistency to find an optimal solution or near-optimal solution with 78 control variables. The difference of power losses between 1k and 5k iterations is only 0.023 which reflect the robustness and stability of AEO optimizeras an effective and reliable optimization solver.

Table 5. Comparison of loss reduction percentage for IEEE 118-bus test system

Algorithms	Case 0	PSO	WCA	CLPSO	GSA	OGSA	CPVEIH-BMO	DE
P_{Loss} MW	132.86	131.99	131.83	130.96	127.76	126.99	124.098	122.36
Loss reduction (%)	–	0.66	0.77	1.43	3.84	4.42	6.60	7.90
Algorithms	**WOA**	**NGBWCA**	**ABC**	**GWO**	**ALO**	**GA**	**MFO**	**AEO**
P_{Loss} MW	122.39	121.47	120.42	120.65	119.77	119.30	116.42	**115.30**
Loss reduction (%)	7.88	8.57	9.33	9.19	9.85	10.95	12.37	**13.21**

Bold values denote the best results.

Case 2: VD minimization

In this case, the minimum, average, and maximum results of active power losses achieved by AEO, NBA and ALO and some other algorithm reported in the literature are tabulated in Table 6. Due to the space reasons, the corresponding optimal control variables of this case are not listed in the paper. The value of VD for AEO is better than other optimizers. From Table 6, it can be pointed that proposed AEO is able to reduce the voltage deviation index by 86.8% with respect to initial losses, compared to 86.7 % with QOTLBO, 84.1 % with TLBO, 72.7 % with PSO-TVAC, 85.5% with SPSO-TVAC, and 83.6 % with PGSWT-PSO. The voltage profiles of all load buses-(PQ buses) for this case are depicted in Fig. 8. It is clear from this figure that the voltage profile has been significantly improved. In case 2, the active power loss is slightly increased to 155.94 MW, while the VD is reduced from 3.41 to 0.1898 p.u, compared with case 1.

Table 6 Comparison of voltage deviation minimization percentage for IEEE 118-bus system

Algorithms	PSO-TVIW [37]	PSO-TVAC [37]	SPSO-TVAC [37]	PGSWT-PSO [37]	TLBO [34]	QOTLBO [34]	AEO
Min VD	0.1935	0.3921	0.2074	0.2355	0.2237	0.1910	**0.1898**
Average VD	0.2291	0.4724	0.2498	0.2755	0.2306	0.2043	**0.2122**
Max VD	0.2809	0.5407	0.3012	0.3239	0.2543	0.2267	**0.2346**
Standard deviation	0.0206	0.0316	0.0215	0.0205	0.0384	0.0356	**0.0117**
P_{Loss}	176.45	179.79	146.81	150.5609	NA	NA	**155.94**
L-max	0.0672	0.0667	0.0650	0.0671	NA	NA	**0.0672**

Bold result denote the best findings

5.3 Large-scale test system IEEE 300-bus [11] : To examine the scalability of the proposed AEO algorithm in solving large-scale ORPD problem, the IEEE 300-bus has been also

analyzed [27][28]. This system consists of sixty-nine generators, forty hundred eleven transmission-lines of which hundred-seven branches with off nominal tap ratios, and fourteen parallel reactive power sources [11]. The total load is (235.258 + j77.8797) p.u. The limits of the control variables are given in Table 2 and from [38]. This test system exhibits very large voltage drops [39], making it harder to ensure the feasibility of solutions. Two cases are considered with this test system:

Case 3: minimization of P_{Loss};

Case 4: Voltage Deviation (VD).

Due to numerous variables and/or for sake of brevity, only the optimal solutions of reactive powers of the best results of three implemented algorithms are presented in the Table 7. From this table, it can be observed that reactive powers of parallel compensators are within admissible limits. The results demonstrates that applying AEO algorithm has led to highest reduction of power loss up to 10.62% compared with that achieved by other solvers, which is to 5.19% with ALO and 3.45% with NBA. Fig. 10 illustrates a comparison between voltage profiles of case 3 and case 4. It is clear from this figure that voltage profile has been significantly improved while guarantying the feasibility of solutions. The convergence plots of the algorithms are shown in Fig. 11, AEO algorithm has better convergence rate compared with NBA and ALO algorithms. Hence, it can be concluded that AEO algorithm has the best performance among all rival techniques.

Table. 7 Reactive power outputs of reactive power sources for IEEE 300-bus system

Reactive power sources	Q_{min} MW	Q_{max} MW	ALO	NBA	AEO
$\mathbf{Q_{96}}$	0	450	156.1047	310.5364	265.9470
$\mathbf{Q_{99}}$	0	59	42.3299	46.6332	56.0155
$\mathbf{Q_{133}}$	0	59	43.1910	13.6233	13.7380
$\mathbf{Q_{143}}$	−450	0	−366.3272	−213.1504	−138.9393
$\mathbf{Q_{145}}$	−450	0	−313.4199	−22.31805	−0.011484
$\mathbf{Q_{152}}$	0	59	26.7216	24.8115	27.3465
$\mathbf{Q_{158}}$	0	59	1.7599	29.6067	50.6618
$\mathbf{Q_{169}}$	−250	0	−43.947	−65.5245	−190.8406
$\mathbf{Q_{210}}$	−450	0	−441.0207	−206.2088	−171.7650
$\mathbf{Q_{217}}$	−450	0	−125.9645	−242.5776	−144.7891
$\mathbf{Q_{219}}$	−150	0	−17.3397	−26.4242	−52.5704
$\mathbf{Q_{227}}$	0	59	11.8801	52.9413	43.0150
$\mathbf{Q_{268}}$	0	15	10.4662	2.5657	2.8092
$\mathbf{Q_{283}}$	0	15	7.7908	3.8356	7.37052
min P_{Loss} MW	P_{Loss}^{0} = 408.316		387.1207	394.2322	**364.9162**

L-index (p.u)	$L_{\text{-index}}{}^{0}$ = 0.4135	0.40816	0.3900	**0.38952**
Reduction Power losses (%)		5.19	3.45	**10.62**

Table 8. Comparison of the results for case 3 of IEEE 300-bus system

Algorithms	MVMO [31]	DEEPSO [31]	SOS [38]	A-CSOS [38]	Gradient Method	ALO	NBA	AEO
Case 3: P_{Loss} minimization								
Min P_{Loss} (MW)	385.62	394.434	409.964	367.1255	372.26	384.922	394.2322	**364.9162**
L-index	NA	NA	NA	NA	NA	0.3663	0.3900	**0.3895**
Reduction *(%)*	5.55	3.4	–0.40	10.08	8.83	5.72	3.44	**11.32**
Case 4: VD minimization								
	SOS [38]		A-CSOS [38]		NBA	ALO		AEO
Min VD (p.u)	4.5420		2.7113		3.8929	3.5033		**1.9718**
P_{Loss} (MW)	NA		NA		553 .168	469.533		**423.243**
L-index	NA		NA		0.4177	0.3945		**0.4045**
Reduction *(%)*	16.33		50.05		28.28	35.46		**63.67**

Table 8, summarizes the comparison results of optimum power losses and voltage deviation obtained by employing different algorithms for both cases. From Table 8 we can see that proposed AEO achieve high quality solutions compared to other approaches. Again, according to numerical findings, lower voltage deviation value by AEO in comparison with other algorithms is observable which achieved to 1.97 (p.u), i.e., minimized by 63.7% compared to the initial value, whereas, is minimized up to 50% with ASOS, 16.3% [38] with SOS, 35.4% [38] with ALO, and 28.28% with NBA. Consequently, proposed AEO algorithm not only benefits from high quality solutions, but also by guarantee the feasibility of solutions of both cases for large-scale test system.

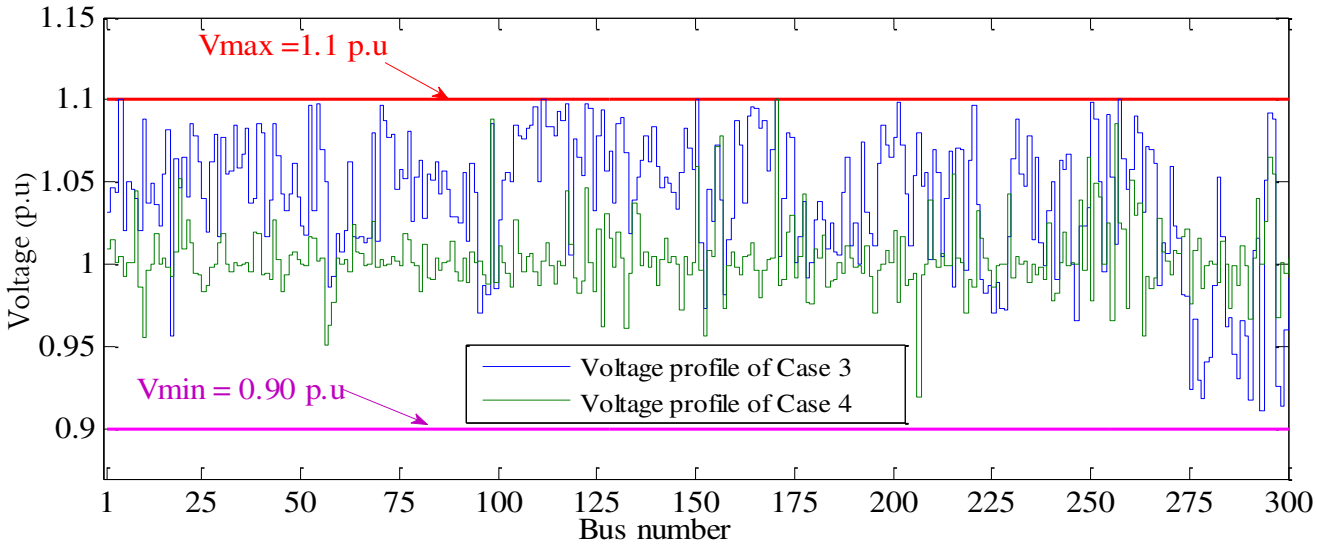

Fig. 10. Voltage profile for both cases of IEEE 300-bus test system

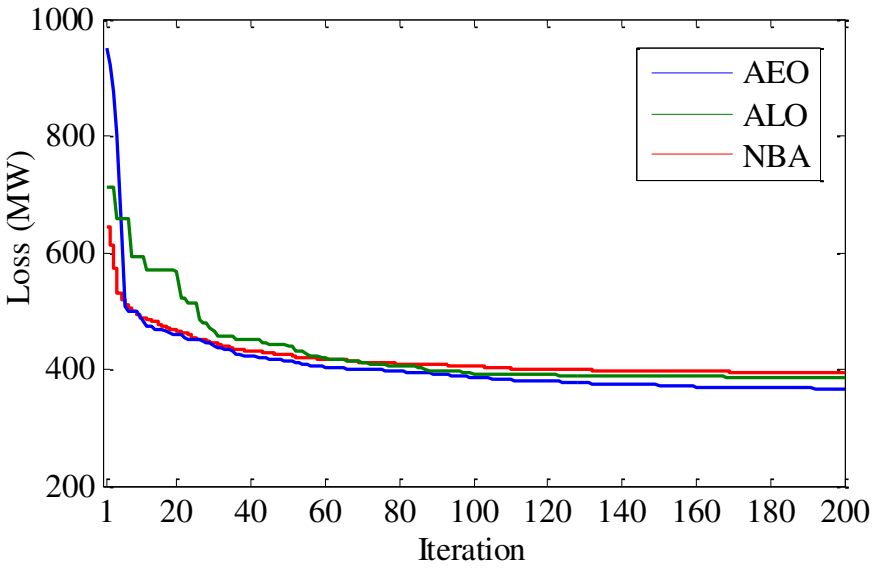

Fig. 11. Comparative convergence curves for P_{Loss} minimization of the 300-bus system

5.4 Algerian electricity grid DZA 114-bus

In order to give a practicability aspect, the Algerian electricity grid DZA 114-bus [29] has been considered as test system. The Algerian electricity grid topology is depicted in Fig. A in the Annex. This system comprises 175 transmissions lines, 15 generators, and 16 branches with off-nominal tap ratio. In addition, buses nos. 50, 55, 66, 67, 77, 89 and 93 have been selected as reactive power sources. The total load demand is (37.27+ j 20.70) p.u at 100 MVA base. Bus 4 is selected as the slack-bus. Therefore, the system has a total of 38 variables to be optimized, including fifteen generators, 16 transformers and seven reactive power sources. Also, this power system presents undesirable voltage drops. The upper and the lower operating limits of the control variables are given in Table 2.

5.4.1 Case 5: minimization of P_{Loss}

Table 9 summarizes the optimal control variables of DZA 114-bus, obtained by AEO, NBA and ALO. From the results, the smallest active power losses are obtained using the AEO technique. The proposed algorithm can find the losses as 53.204 MW in continuous variables case and 53.244 MW with discrete variables case. The results confirm that the AEO algorithm is able to find the best solution for both kinds of control variables (continuous and discrete) in comparison to the results of NBA and ALO algorithms. The evolution of losses across iterations for three algorithms are given in Fig. 12. The performance of AEO for 30 independent execution runs is shown in Fig. 13. From this figure, it can be seen that the

difference between worst and best solution not exceed 1.61 MW. It can be observed that best, worst solutions for all test systems after 30 runs are extremely close, which clearly reflects the stability and robustness of AEO algorithm in terms of exploring the optimal solution in each trial.

Table 9. Solution of minimum power losses (MP) for Algerian Electricity Grid DZA 114-bus

Control variables	*Continuous variables*				*Discrete variables*		
	ALO	**NBA**	**AEO**		**ALO**	**NBA**	**AEO**
Case 5							
Generator Voltage (p.u)							
$\mathbf{V_4}$	1.099960	1.1	1.099999		1.1	1.099994	1.1
$\mathbf{V_5}$	1.099750	1.1	1.099833		1.099999	1.099562	1.0997
$\mathbf{V_{11}}$	1.096232	1.1	1.099999		1.099981	1.099991	1.1
$\mathbf{V_{15}}$	1.093981	1.098069	1.091310		1.098029	1.092537	1.0935
$\mathbf{V_{17}}$	1.1	1.1	1.099999		1.1	1.1	1.0999
$\mathbf{V_{19}}$	1.055576	1.066200	1.082310		1.017579	1.022780	1.0936
$\mathbf{V_{22}}$	1.062448	1.071543	1.087102		1.023613	1.020059	1.0985
$\mathbf{V_{52}}$	1.042803	1.050259	1.087556		1.023684	1.032393	1.0932
$\mathbf{V_{80}}$	1.093085	1.091932	1.091039		1.098850	1.091589	1.0926
$\mathbf{V_{83}}$	1.099997	1.099171	1.099837		1.1	1.1	1.0999
$\mathbf{V_{98}}$	1.0995280	1.099086	1.099271		1.099999	1.1	1.1
$\mathbf{V_{100}}$	1.1	1.1	1.099995		1.1	1.099999	1.0999
$\mathbf{V_{101}}$	1.1	1.1	1.1		1.1	1.099745	1.0999
$\mathbf{V_{109}}$	1.0998462	1.1	1.099947		1.1	1.099999	1.1
$\mathbf{V_{111}}$	1.0975876	1.1	1.099976		1.1	1.099286	1.1
Tap ratio (p.u)							
$\mathbf{T_{80\text{-}81}}$	1.0074685	1.039184	0.901745		1.03	0.99	0.90
$\mathbf{T_{81\text{-}90}}$	1.0581378	1.029146	0.946162		1.04	1.04	0.96
$\mathbf{T_{86\text{-}93}}$	1.0735973	1.015320	0.963416		1.05	1.06	0.99
$\mathbf{T_{42\text{-}41}}$	1.0668528	1.013559	0.980564		1.04	1.08	0.98
$\mathbf{T_{58\text{-}57}}$	1.0716278	0.993079	0.965906		1.07	1.02	0.97
$\mathbf{T_{44\text{-}43}}$	1.0878220	1.022719	0.974318		1.05	1.06	1.00
$\mathbf{T_{60\text{-}59}}$	1.0518370	1.044176	0.989930		1.08	1.03	0.98
$\mathbf{T_{64\text{-}63}}$	1.0938053	0.973303	0.959374		1.03	1.02	0.97
$\mathbf{T_{72\text{-}71}}$	1.0395981	0.982745	0.955683		1.01	1.06	0.96
$\mathbf{T_{17\text{-}18}}$	1.0023307	0.994556	0.989024		1.05	1.03	0.98
$\mathbf{T_{21\text{-}20}}$	1.0379620	1.022736	0.998976		1.09	1.05	0.99
$\mathbf{T_{27\text{-}26}}$	1.0416436	0.975391	0.961404		1.09	1.03	0.96
$\mathbf{T_{28\text{-}26}}$	1.0933018	1.050337	1.029924		1.06	1.06	1.02
$\mathbf{T_{31\text{-}30}}$	1.0676910	1.027098	0.989257		1.04	1.05	0.99
$\mathbf{T_{48\text{-}47}}$	1.0972839	1.024613	0.984472		1.09	1.1	0.99
$\mathbf{T_{74\text{-}73}}$	1.0648045	0.948207	1.014127		1.08	1.07	1.08
Capacitor Banks (MVAR)							
$\boldsymbol{Q_{C\text{-}50}}$	22.509200	16.09386	24.35864		13	24	25
$\boldsymbol{Q_{C\text{-}55}}$	14.801860	12.77946	10.15448		23	15	10
$\boldsymbol{Q_{C\text{-}66}}$	24.509874	24.32149	19.44356		18	23	22
$\boldsymbol{Q_{C\text{-}67}}$	21.278427	20.83231	25		19	25	25
$\boldsymbol{Q_{C\text{-}77}}$	23.289257	20.41054	14.309846		24	25	16
$\boldsymbol{Q_{C\text{-}89}}$	21.607676	8.110358	7.539387		21	15	7

$Q_{C\text{-}93}$	24.973281	25	24.95138		13	25	25
P_{Loss} (MW)	57.02444	55.122041	**53.2043026**		57.412317	55.9677	**53.244609**
L-index	0.312056	0.31199	**0.278219**		0.315175	0.302761	**0.278153**
P_{save} (%)	15.4	18.27	**21.11**		14.8	17	**21**
Case 6							
Algorithms	**ALO**	**NBA**	**AEO**		**ALO**	**NBA**	**AEO**
VD (p.u)	1.2179	1.28439	**1.04515**		1.2183	1.43166	**1.07067**
P_{Loss} (MW)	65.611	74.478	**71.779**		66.710	75.592	**72.679**
L-index	0.3233	0.3177	**0.31822**		0.31817	0.319307	**0.31791**

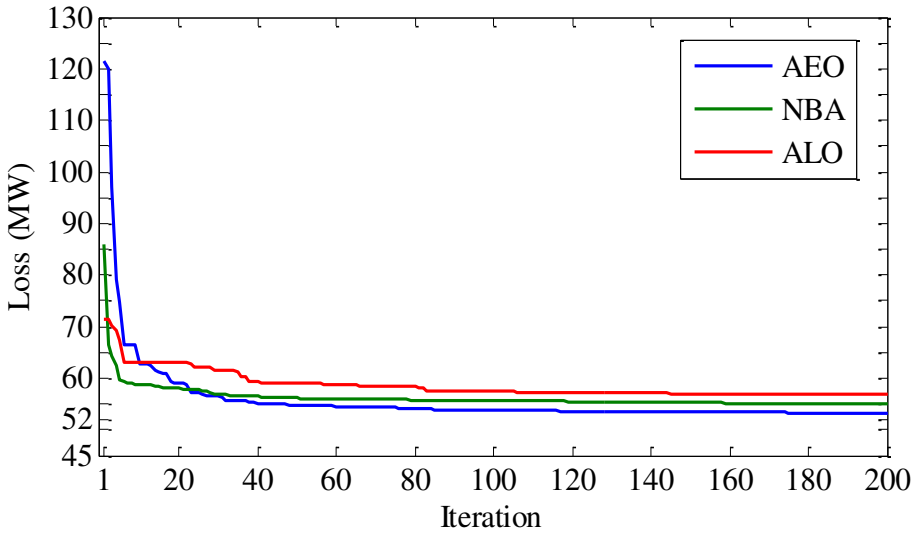

Fig. 12. Comparative convergence curves for P_{Loss} minimization of the DZA 114-bus

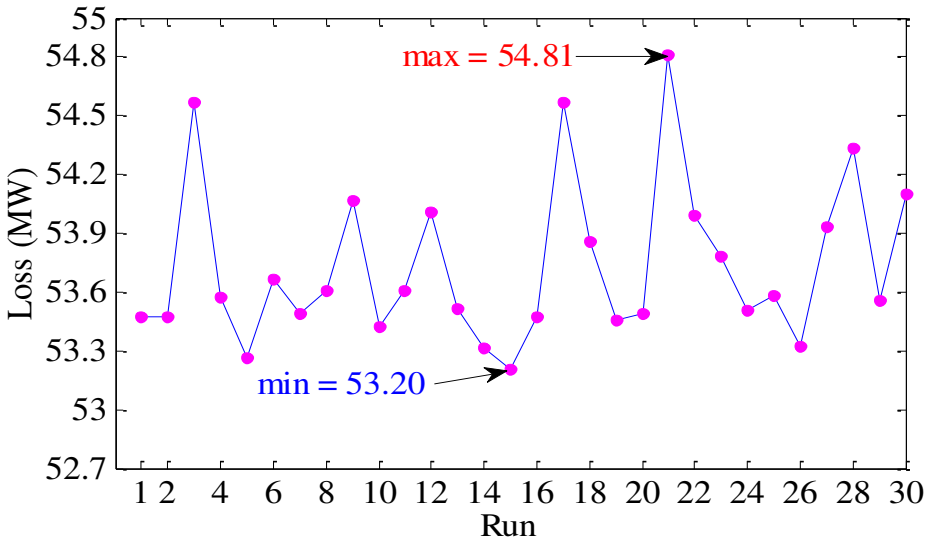

Fig. 13. Performance of 30 individuals for 30 independent execution runs

5.4.2 Results of DZA 114-bus when increasing iterations number to 1k, 10k and 50 k

Simulation results obtained when enlarging iteration numbers by 1k, 10k and 50k for practical power system DZA114-bus are reported in Table 9.1. From this table, we can see that active power losses value is no variation with enlarging number of iterations from 1k, 10k to 50k times, which reflect the robustness and stability of AEO optimizer as an effective and reliable optimization solver. Moreover, AEO is more efficient than other optimizer. The success of AEO algorithm depends on having good balance between exploration and exploitation abilities, in which after a sufficient number of iterations AEO algorithm converge to the same value, and any enlargement in the iterations does not improve the performance of the AEO algorithm significantly.

Table 9.1 Results of DZA114-bus vs. iteration numbers

Algorithms	**NBA**			**ALO**			**AEO**		
Iteration	1k	10k	50k	1k	10k	50k	1k	10k	50k
$\mathbf{P_{Loss}}$ (MW)	53.236	52.977	52.894	56.249	56.047	54.725	52.735	52.734	52.734
VD	6.5402	6.6713	6.9042	3.1059	3.700	5.1769	6.9547	6.9543	6.8913
L-index	0.2782	0.2781	0.2781	0.3032	0.3089	0.2781	0.2782	0.2781	0.2781

5.4.3 Case 6 Voltage deviation minimization (VD)

In this case, the proposed algorithm is also applied to minimize the total voltage deviation. Case 6 of Table 9 gives the simulation results obtained by three algorithms with either discrete or continuous variables. The VD value obtained by the AEO algorithm is better than those accomplished by the NBA and ALO algorithms for both kinds of variables. It can be seen that also with discrete control variables AEO converge to the optimal solutions. In case 6, the active power losses is slightly increased, while the voltage deviation VD is reduced from 7.024 to 1.045 with continuous variables and from 6.84 p.u to 1.07067 p.u with discrete variables compared with case 5, respectively. For ALO and NBA algorithms the optimized voltage deviation is 1.2179 and 1.28439 p.u, for continuous variables and 1.2183 and 1.43166 p.u, for discrete variables. Hence, it can be drawn that AEO algorithm is better than all other listed algorithms in terms global search capacity and efficacy to solve large-sized and nonlinear optimization problems. Fig. 14 presents a comparison between voltage profiles of case 5 and case 6 for Algerian electricity grid DZA 114-bus. It can be seen that all bus voltage magnitudes are within the admissible limits.

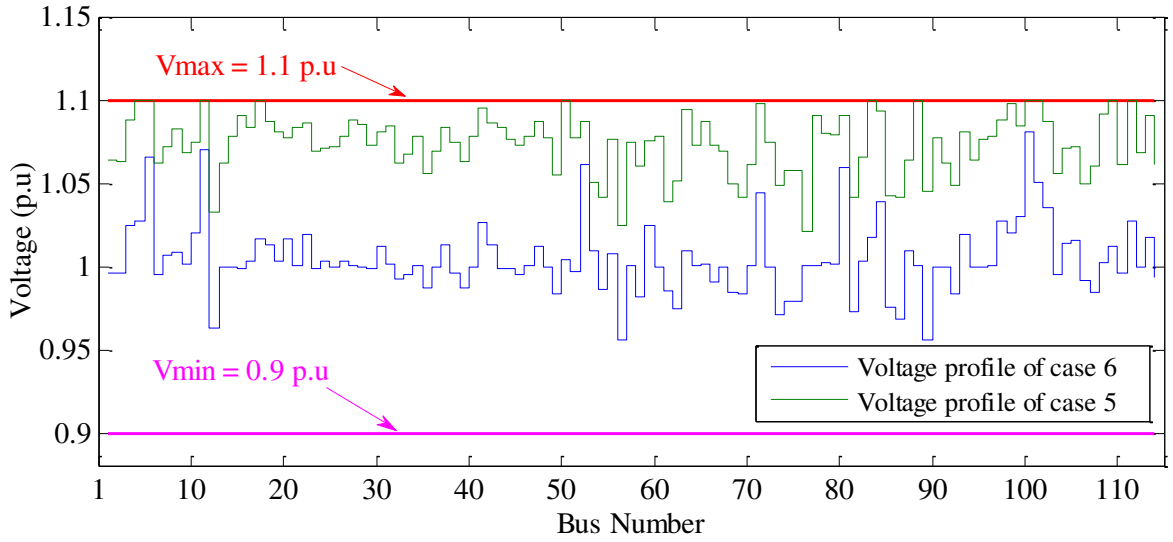

Fig. 14. Voltage profile for DZA 114-bus power system

5.5 Statistical test of one-way ANOVA

Due to the stochastic nature of meta-heuristic optimization algorithms, it is evident must be run each technique several times on the same objective function in an effort to get the best result values, which probably vary to each execution. Instead of relying on the statistics of the aforementioned results in terms of best, worst solution and standard deviation, one-way analysis of variance (ANOVA) has been performed to observe the statistical significance of the difference between the performance of AEO algorithm and other implemented approaches. This study gives certain level of confidence to the present work 95% and to evaluate which techniques could be potentially suitable to cope with ORPD problem in large-scale systems. The one-way ANOVA results obtained from experimented algorithms on three test systems (IEEE 30-bus, IEEE 118-bus and DZA 114-bus) are listed in Table 10.

Table 10 One way ANOVA stats for active power losses of IEEE 30-bus system

Null hypothesis	All means are equal
Alternative hypothesis	At least one mean is different
Significance level	$\alpha = 0.05$

Test ANOVA IEEE 30-bus

Source of variance	SS	df	MS	F	P-value	F-crit
Between groups	0.18868	2	0.09434	136.23	1.5785 e-27	3.1012
Within groups	0.06025	87	0.00069			
Total	0.24893	89				

Test ANOVA IEEE 118-bus

Source of variance	SS	df	MS	F	P-value	F-crit
Between groups	956.14	2	478.07	205.69	1.0604 e-33	3.1012
Within groups	202.21	87	2.324			
Total	1158.35	89				

Test ANOVA DZA 114-bus

Source of variance	SS	df	MS	F	P-value	F-crit
Between groups	209.827	2	104.914	77.18	5.2785 e-20	3.1012
Within groups	118.256	87	1.359			
Total	328.083	89				

Table 10 lists results of one way ANOVA test. In this experiment, assumption of homogeneous variances is considered, it can be seen that the p-value is less than significance level of 0.05. It can be declared that the null hypothesis can be rejected. There is statistically significant difference between the means of the different groups. Thus, it is strong evidence that the mean values in the groups differ. Hence AEO is statistically different from ALO and NBA. Results of statistics, in term of minimum P_{loss}, learning curves for the best (minimum P_{loss}), average (mean P_{loss}), and worst (maximum P_{loss}) histogram studies, and box plot presentations, are illustrated in Figures 16, 17, and 18 for IEEE 30-bus, IEEE 118-bus, and DZA 114-bus. The learning-curves for the best, average and worst as presented in figures. 17a and 18a show that consistent iterative optimization of fitness functions is achieved by AEO and even worst case gives the lowest power losses compared to the base case, which endorsed the accurate optimization of proposed AEO. The box plot illustrations are presented in Figs. 16b, 17b and 18b for three test systems IEEE 30-bus, IEEE 118-bus and DZA 114-bus, respectively.

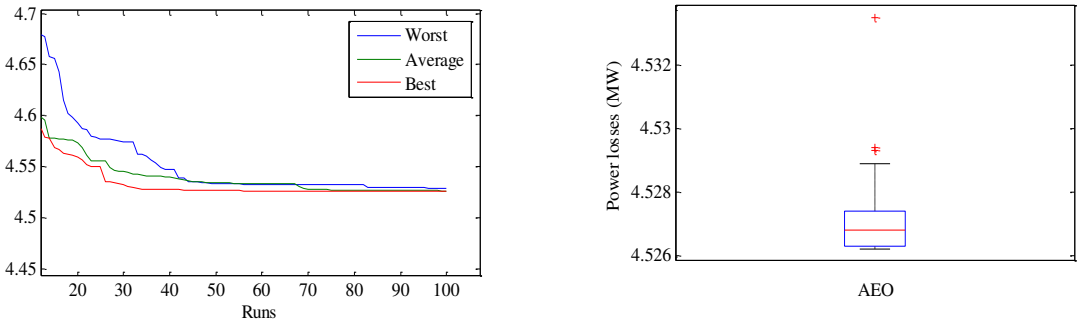

(a) Learning curves (b) Fitness box-plot

Figure 16. Statistical analysis of ORPD for IEEE 30-bus

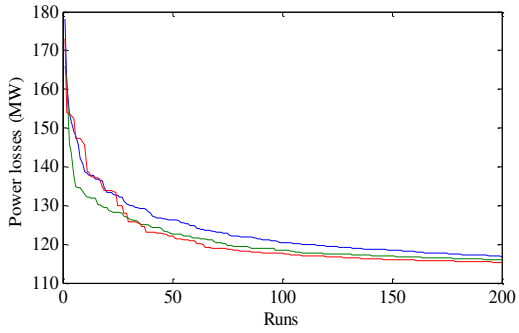

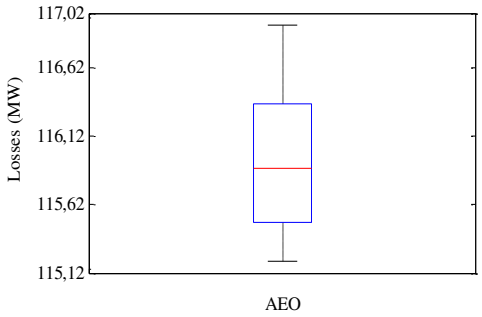

(a) Learning curves (b) Fitness box-plot

Figure 17. Statistical analysis of ORPD for IEEE 118-bus

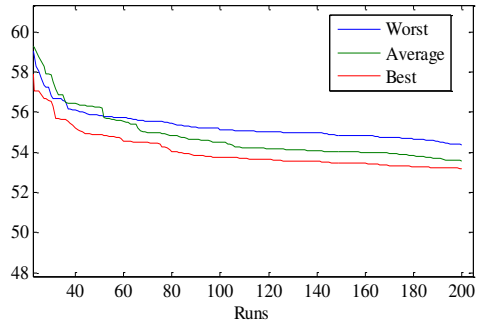

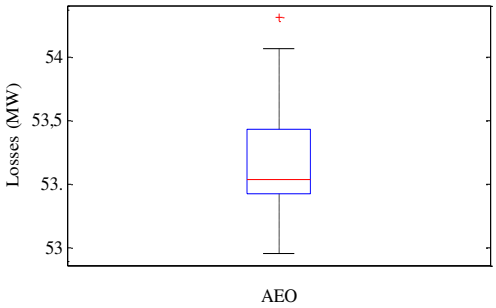

(a) Fitness box-plot (b) Fitness box-plot

Figure 18. Statistical analysis of ORPD for DZA114-bus

6. Conclusions

This paper proposed AEO, a newly introduced optimization paradigm, for solving the nonlinear ORPD problems in the practical and large-scale power systems by finding optimal values of control variables to minimize active power losses and improving voltage profile index. The proposed technique has been improved to deal with the mixed-type control variables (continuous and discrete) of problem. The performance of proposed AEO algorithm were examined on medium- and large-scale test systems (IEEE 30-bus, IEEE 118-bus, IEEE 300-bus), as well as on the practical Algerian power system DZA 114-bus, Six cases of single objective ORPD are solved via three solvers, such as: minimization of active power losses, voltage deviation minimization as well as minimization of voltage stability index. Comparison of the proposed findings with other state of the art meta-heuristic techniques indicates that the given scheme outperformed its counterparts in all objective functions. Results of statistics in terms of learning curves, one way ANOVA test and probability plots based on 30 independent trials of AEO for practical power system show the consistency, robustness and stability of the AEO algorithm as an alternative, accurate and effective

optimization technique. The complexity of AEO for the solutions of IEEE 30-bus and IEEE 118-bus systems for 30 independent runs shows that in case of small-sized test system IEEE 30-bus with 25 control variables, there is no noticeable difference observed, while in case of IEEE 118-bus system with 78 control variables, the complexity indices are on higher side which is understandable because the optimization problem become stiffer with increase in the degrees of freedom.

At the end, on the light of detailed information given in this article, it is concluded that the suggested algorithm is the more suitable choice of coping optimal reactive power dispatch problems where it prove its efficiency even with large-scale and real power systems. More importantly, the proposed optimizer is eligible to sustain the solution feasibility.

In future, the proposed optimization paradigm AEO looks promising for finding the solution of paramount signification application arising in plasma physics [41,42], astrophysiques [43,44], atomic physics [45,46], nuclear physics [47] circuit theory [48], financial modelling [49,50], energy [51,52], and fluid dynamics [53].

Acknowledgement

We gratefully acknowledge the support of the Algerian electricity company SONELGAZ.

This work was supported in part by the Exceptional National Program of Algeria PNE 2019/2020 and the Key Program of Fundamental Research of Electrical Engineering Department at Jaen University, Spain 2020.

Conflict of Interest and Authorship Conformation Form

- Conflict of interest: All authors declared that there are no potential conflicts of interest.
- Human and animal rights All authors declared that there is no research involving human and/or animal.
- All authors have participated in (a) conception and design, or analysis and interpretation of the data; (b) drafting the article or revising it critically for important intellectual content; and (c) approval of the final version.
- This manuscript has not been submitted to, nor is under review at, another journal or other publishing venue.

- The authors have no affiliation with any organization with a direct or indirect financial interest in the subject matter discussed in the manuscript

References

[1] A.F. Attia, R.A. El Sehiemy, H.M. Hasanien, Optimal power flow solution in power systems using a novel Sine-Cosine algorithm, Int. J. Electr. Power Energy Syst. 99 (2018) 331–343.

[2] Warid Warid, Optimal power flow using the AMTPG-Jaya algorithm, Appl. Soft Comput. J. 91 (2020) 106252.

[3] P.P. Biswas, P.N. Suganthan, R. Mallipeddi, G.A.J. Amaratunga, Optimal power flow solutions using differential evolution algorithm integrated with effective constraint handling techniques, Eng. Appl. Artif. Intell. 68 (2018) 81–100.

[4] V.H. Hinojosa, R. Araya, Modeling a mixed-integer-binary small-population evolutionary particle swarm algorithm for solving the optimal power flow problem in electric power systems, Appl. Soft Comput. 13 (2013).

[5] T.L. Duong, M.Q. Duong, V.D. Phan, T.T. Nguyen, A. Niccolai, Optimal Reactive Power Flow for Large-Scale Power Systems Using an Effective Metaheuristic Algorithm, J. Electr. Comput. Eng. Article ID 6382507 (2020).

[6] T.T. Nguyen, D.N. Vo, H. Van Tran, L. Van Dai, Optimal Dispatch of Reactive Power Using Modified Stochastic Fractal Search Algorithm, Complexity. Article ID 4670820 (2019).

[7] G. Chen, L. Liu, Z. Zhang, S. Huang, Optimal reactive power dispatch by improved GSA-based algorithm with the novel strategies to handle constraints, Appl. Soft Comput. J. 50 (2017) 58–70.

[8] M. Ghasemi, M. Taghizadeh, S. Ghavidel, J. Aghaei, A. Abbasian, Solving optimal reactive power dispatch problem using a novel teaching-learning-based optimization algorithm, Eng. Appl. Artif. Intell. 39 (2015) 100–108.

[9] A.R.J. Ali Asghar Heidari, Rahim Ali Abbaspour, Gaussian bare-bones water cycle algorithm for optimal reactive power dispatch in electrical power systems, Appl. Soft Comput. J. 57 (2017) 657–671.

[10] E. Naderi, H. Narimani, M. Fathi, M.R. Narimani, A Novel Fuzzy Adaptive Configuration of Particle Swarm Optimization to Solve Large-Scale Optimal Reactive

Power Dispatch, Appl. Soft Comput. J. 53 (2017) 441–456.

[11] S. Mouassa, T. Bouktir, A. Salhi, Ant lion optimizer for solving optimal reactive power dispatch problem in power systems, Eng. Sci. Technol. an Int. J.20 (2017) 885–895.

[12] S. Mouassa, T. Bouktir, Multi-objective ant lion optimization algorithm to solve large-scale multi-objective optimal reactive power dispatch problem, COMPEL - Int. J. Comput. Math. Electr. Electron. Eng. 38 (2018) 305–322.

[13] S. Mouassa, T. Bouktir, Artificial Bee Colony Algorithm for Discrete Optimal Reactive Power Dispatch, Proc. 2015 Int. Conf. Ind. Eng. Syst. Manag. IEEE IESM 21-23 Oct. 2015. (2015). 10.1109/IESM.2015.7380228

[14] R. Ng, S. Mei, M. Herwan, Z. Mustaffa, H. Daniyal, Optimal reactive power dispatch solution by loss minimization using moth-flame optimization technique, Appl. Soft Comput. J. 59 (2017) 210–222.

[15] M.H. Sulaiman, Z. Mustaffa, M.R. Mohamed, O. Aliman, Using the gray wolf optimizer for solving optimal reactive power dispatch problem, Appl. Soft Comput. J. 32 (2015) 286–292.

[16] D. Gutiérrez, J.M. López, W.M. Villa, Metaheuristic Techniques Applied to the Optimal Reactive Power Dispatch: A Review, IEEE Lat. Am. Trans. 14 (2016) 2253–2263.

[17] M.S. Saddique, A.R. Bhatti, S.S. Haroon, M.K. Sattar, S. Amin, I.A. Sajjad, S.S. ul Haq, A.B. Awan, N. Rasheed, Solution to optimal reactive power dispatch in transmission system using meta-heuristic techniques—Status and technological review, Electr. Power Syst. Res. 178 (2020) 106031.

[18] Y. Muhammad, R. Khan, M. Asif, Z. Raja, F. Ullah, Solution of optimal reactive power dispatch with FACTS devices : A survey, 6 (2020) 2211–2229.

[19] S. Li, W. Chen, S. Li, K.S. Leung, Improved algorithm on online clustering of bandits, IJCAI Int. Jt. Conf. Artif. Intell. 2019-August (2019) 2923–2929.

[20] S. Li, A. Karatzoglou, C. Gentile, Collaborative filtering bandits, SIGIR 2016 - Proc. 39th Int. ACM SIGIR Conf. Res. Dev. Inf. Retr. (2016) 539–548.

[21] N. Korda, B. Szorenyi, S. Li, Distributed clustering of linear bandits in peer to peer networks, 33rd Int. Conf. Mach. Learn. ICML 2016. 3 (2016) 1966–1980.

[22] K. Mahadik, Q. Wu, S. Li, A. Sabne, Fast distributed bandits for online recommendation systems, Proc. Int. Conf. Supercomput. (2020).

[23] P. Kar, S. Li, H. Narasimhan, S. Chawla, F. Sebastiani, Online optimization methods

for the quantification problem, Proc. ACM SIGKDD Int. Conf. Knowl. Discov. Data Min. 13-17-August-2016 (2016) 1625–1634. doi:10.1145/2939672.2939832.

[24] A.A.A. El Ela, M.A. Abido, S.R. Spea, Differential evolution algorithm for optimal reactive power dispatch, Electr. Power Syst. Res. 81 (2011) 458–464. doi:10.1016/j.epsr.2010.10.005.

[25] P. Kessel, H. Glavitsch, Estimating the voltage stability of a power system, IEEE Trans. Power Deliv. 1 (1986) 346–354. doi:10.1109/TPWRD.1986.4308013.

[26] W. Zhao, L. Wang, Artificial ecosystem-based optimization : a novel nature-inspired meta-heuristic algorithm, Springer London, 2019.

[27] R.D. Zimmerman, C.E. Murillo Sánchez, R.J. Thomas, MATPOWER: Steady-State Operations, Planning, and Analysis Tools for Power Systems Research and Education, Power Syst. IEEE Trans. 26 (2011) 12–19. doi:10.1109/TPWRS.2010.2051168.

[28] A.P. Mazzini, S. Member, E.N. Asada, Solving Control-Constrained Reactive Power Dispatch with Discrete Variables, (2015).

[29] Y. Amrane, M. Boudour, M. Belazzoug, A new Optimal reactive power planning based on Differential Search Algorithm, Int. J. Electr. Power Energy Syst. 64 (2015) 551–561. doi:10.1016/j.ijepes.2014.07.060.

[30] A. Rajan, T. Malakar, Optimal reactive power dispatch using hybrid Nelder-Mead simplex based firefly algorithm, Int. J. Electr. Power Energy Syst. 66 (2015) 9–24. doi:10.1016/j.ijepes.2014.10.041.

[31] K.Y. Lee, Y.M. Park, J.L. Ortiz, A United Approach to Optimal Real and Reactive Power Dispatch, IEEE Power Eng. Rev. PER-5 (1985) 42–43. doi:10.1109/MPER.1985.5526580.

[32] S. Duman, Y. Sönmez, U. Güvenç, N. Yörükeren, Optimal reactive power dispatch using a gravitational search algorithm, IET Gener. Transm. Distrib. 6 (2012) 563. doi:10.1049/iet-gtd.2011.0681.

[33] S. Mouassa, T. Bouktir, A. Salhi, Ant lion optimizer for solving optimal reactive power dispatch problem in power systems, Eng. Sci. Technol. an Int. J. 20 (2017). doi:10.1016/j.jestch.2017.03.006.

[34] B. Mandal, P.K. Roy, Optimal reactive power dispatch using quasi-oppositional teaching learning based optimization, Int. J. Electr. Power Energy Syst. 53 (2013) 123–134. doi:10.1016/j.ijepes.2013.04.011.

[35] O.B. Optimization, A. Bhattacharya, Solution of Optimal Reactive Power Flow using,

4 (2010) 26–34.

[36] B. Shaw, V. Mukherjee, S.P. Ghoshal, Solution of reactive power dispatch of power systems by an opposition-based gravitational search algorithm, Int. J. Electr. Power Energy Syst. 55 (2014) 29–40. doi:10.1016/j.ijepes.2013.08.010.

[37] J. Polprasert, W. Ongsakul, V.N. Dieu, Optimal Reactive Power Dispatch Using Improved Pseudo-gradient Search Particle Swarm Optimization, Electr. Power Components Syst. 44 (2016) 518–532. doi:10.1080/15325008.2015.1112449.

[38] E. Yalçın, E. Çam, M.C. Taplamacıoğlu, A new chaos and global competitive ranking ‐ based symbiotic organisms search algorithm for solving reactive power dispatch problem with discrete and continuous control variable, Electr. Eng. 102 (2020) 573–590. doi:10.1007/s00202-019-00895-6.

[39] C. Coffrin, D. Gordon, P. Scott, NESTA, The NICTA Energy System Test Case Archive, ArXiv1411.0359 [Cs]. (2014) 1–26. http://arxiv.org/abs/1411.0359%5Cnhttp://www.arxiv.org/pdf/1411.0359.pdf.

[40] R. Pinto, Stochastic Location of FACTS Devices in Electric Power Transmission Networks, (2013) 86.

[41] M.A.Z. Raja, M.A. Manzar, F.H. Shah, F.H. Shah, Intelligent computing for Mathieu's systems for parameter excitation, vertically driven pendulum and dusty plasma models, Appl. Soft Comput. J. 62 (2018) 359–372. doi:10.1016/j.asoc.2017.10.049.

[42] A.H. Bukhari, M. Sulaiman, M.A.Z. Raja, S. Islam, M. Shoaib, P. Kumam, Design of a hybrid NAR-RBFs neural network for nonlinear dusty plasma system, Alexandria Eng. J. (2020). doi:10.1016/j.aej.2020.04.051.

[43] I. Ahmad, M.A.Z. Raja, M. Bilal, F. Ashraf, Neural network methods to solve the Lane–Emden type equations arising in thermodynamic studies of the spherical gas cloud model, Neural Comput. Appl. 28 (2017) 929–944. doi:10.1007/s00521-016-2400-y.

[44] Z. Sabir, H.A. Wahab, M. Umar, M.G. Sakar, M.A.Z. Raja, Novel design of Morlet wavelet neural network for solving second order Lane–Emden equation, Math. Comput. Simul. 172 (2020) 1–14. doi:10.1016/j.matcom.2020.01.005.

[45] S. ul I. Ahmad, F. Faisal, M. Shoaib, M.A.Z. Raja, A new heuristic computational solver for nonlinear singular Thomas–Fermi system using evolutionary optimized cubic splines, Eur. Phys. J. Plus. 135 (2020) 1–29. doi:10.1140/epjp/s13360-019-00066-3.

[46] Z. Sabir, M.A. Manzar, M.A.Z. Raja, M. Sheraz, A.M. Wazwaz, Neuro-heuristics for nonlinear singular Thomas-Fermi systems, Appl. Soft Comput. J. 65 (2018) 152–169. doi:10.1016/j.asoc.2018.01.009.

[47] A. Zameer, M. Muneeb, S.M. Mirza, M.A.Z. Raja, Fractional-order particle swarm based multi-objective PWR core loading pattern optimization, Ann. Nucl. Energy. 135 (2020) 106982. doi:10.1016/j.anucene.2019.106982.

[48] A. Mehmood, A. Zameer, M.S. Aslam, M.A.Z. Raja, Design of nature-inspired heuristic paradigm for systems in nonlinear electrical circuits, Neural Comput. Appl. 32 (2020) 7121–7137. doi:10.1007/s00521-019-04197-7.

[49] A.H. Bukhari, M.A.Z. Raja, M. Sulaiman, S. Islam, M. Shoaib, P. Kumam, Fractional neuro-sequential ARFIMA-LSTM for financial market forecasting, IEEE Access. 8 (2020) 71326–71338. doi:10.1109/ACCESS.2020.2985763.

[50] A. Ara, N.A. Khan, O.A. Razzaq, T. Hameed, M.A.Z. Raja, Wavelets optimization method for evaluation of fractional partial differential equations: an application to financial modelling, Adv. Differ. Equations. 2018 (2018) 1–13. doi:10.1186/s13662-017-1461-2.

[51] F. Shahid, A. Zameer, A. Mehmood, M.A.Z. Raja, A novel wavenets long short term memory paradigm for wind power prediction, Appl. Energy. 269 (2020) 115098. doi:10.1016/j.apenergy.2020.115098.

[52] A. Zameer, J. Arshad, A. Khan, M.A.Z. Raja, Intelligent and robust prediction of short term wind power using genetic programming based ensemble of neural networks, Energy Convers. Manag. 134 (2017) 361–372. doi:10.1016/j.enconman.2016.12.032.

[53] M.A.Z. Raja, A. Mehmood, A. ur Rehman, A. Khan, A. Zameer, Bio-inspired computational heuristics for Sisko fluid flow and heat transfer models, Appl. Soft Comput. J. 71 (2018) 622–648. doi:10.1016/j.asoc.2018.07.023.

July 2020 Neural Computing and Applications 32(4):1-43

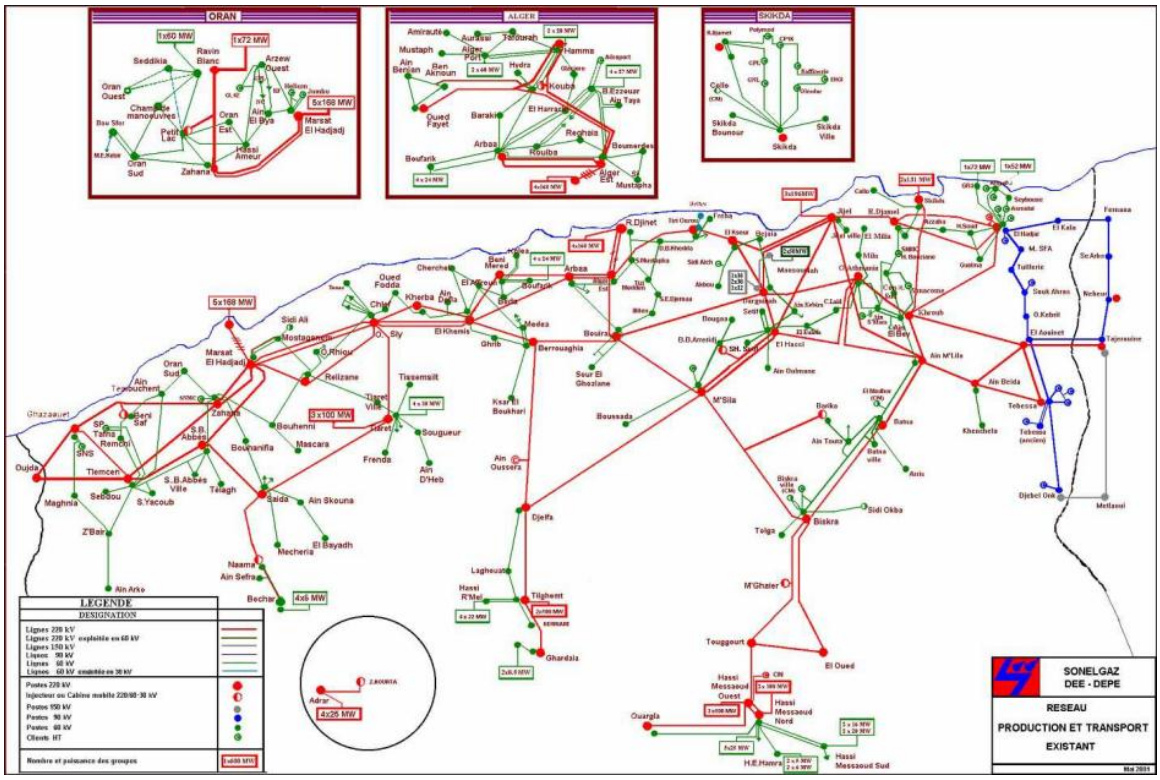

Fig. 15 Algerian electricity grid DZA 114-bus